

## ECMWF forecast performance during the June 2013 flood in Central Europe

T. Haiden, L. Magnusson, I. Tsonevsky,  
F. Wetterhall, L. Alfieri, F. Pappenberger,  
P. de Rosnay, J. Muñoz-Sabater,  
G. Balsamo, C. Albergel, R. Forbes,  
T. Hewson, S. Malardel, D. Richardson

Forecast and Research Departments

June 2014

This paper has not been published and should be regarded as an Internal Report from ECMWF.  
Permission to quote from it should be obtained from the ECMWF.



European Centre for Medium-Range Weather Forecasts  
Europäisches Zentrum für mittelfristige Wettervorhersage  
Centre européen pour les prévisions météorologiques à moyen

Series: ECMWF Technical Memoranda

A full list of ECMWF Publications can be found on our web site under:

<http://www.ecmwf.int/publications/>

Contact: [library@ecmwf.int](mailto:library@ecmwf.int)

© Copyright 2014

European Centre for Medium Range Weather Forecasts  
Shinfield Park, Reading, Berkshire RG2 9AX, England

Literary and scientific copyrights belong to ECMWF and are reserved in all countries. This publication is not to be reprinted or translated in whole or in part without the written permission of the Director. Appropriate non-commercial use will normally be granted under the condition that reference is made to ECMWF.

The information within this publication is given in good faith and considered to be true, but ECMWF accepts no liability for error, omission and for loss or damage arising from its use.

## Abstract

A case of orographically enhanced, extreme precipitation which led to extensive flooding in Central Europe is investigated. The ECMWF Integrated Forecasting System (IFS) provided good forecasts of the location of the heaviest precipitation on the northern side of the Alps but underestimated the magnitude. As a result, streamflow predictions for the Danube by the European Flood Alert System (EFAS) run with ECMWF input underestimated peak discharge values. We investigate possible causes for the underestimation such as model resolution, the microphysical parameterization, and soil moisture in the model. Increasing the model resolution has a substantial positive effect on the magnitude of the predicted rainfall in the worst affected region on the northern side of the Alps. It also improves forecasts over the Czech Republic where an observed, non-orographic band of enhanced precipitation is predicted which was not simulated in the operational forecast. A new parameterization of precipitation formation which will become operational in 2014 is shown to have a positive effect as well, leading to about 10% increase in total precipitation on the northern side of the Alps. Experiments with different options for soil moisture assimilation show little effect since the near-saturated conditions due to positive rainfall anomalies in the weeks prior to the event were already well captured by the soil model in the IFS, even without soil moisture assimilation.

## 1 Introduction

In June 2013 massive flooding hit the Upper Danube and Elbe basins and their tributaries. In Passau, at the confluence of the Inn, Ilz and Danube, water levels reached values not seen since 1501. Further downstream in Vienna, river discharge values exceeded those observed in the past two centuries (Blöschl et al., 2013). Elbe tributaries such as the Saale experienced flooding corresponding to a return period of several hundred years. A total of 25 fatalities in the Czech Republic, Germany, and Austria have been attributed to the flooding.

Owing to the large-scale nature of the event, meteorological and hydrological forecasts were generally good, in particular for the location of maximum precipitation amounts (south-eastern Bavaria). However there was a tendency in the forecasts, especially from global models, to underestimate precipitation amounts. As a result, peak river discharge forecasts based on input from these models were too low. Because of its severity and high impact, this event constitutes an important case study and useful benchmark for improvements in atmospheric and hydrological forecasting systems.

Strong orographic precipitation enhancement along the northern slopes of the Alps was observed during this event, leading to highest rainfall totals on the order of 300-400 mm in 4 days in southern Germany and in Austria (Stein and Malitz, 2013). Orographic effects also played a role in the Czech Republic, where the Sudetes, Ore, and Sumava mountains caused substantial rainfall enhancement (Brozkova et al., 2013). The importance of dynamically forced orographic lifting during flood events in mountain areas is well known, and the high efficiency of precipitation formation in such cases is generally attributed to the seeder-feeder mechanism (e.g. Roberts et al., 2009). This requires a combination of strong, moist low-level flow producing orographic clouds with a low cloud base, and precipitation falling from a higher-level (e.g. frontal) cloud which efficiently accretes the orographically generated and continuously replenished cloud water. Both ingredients were in place for a period of several days during the June 2013 event.

Forecasts of orographic precipitation enhancement are sensitive to horizontal resolution because to first order rainfall amounts are proportional to terrain slope. Westrick and Mass (2001) note an increase by about 25% of precipitation totals during a flood event in the coastal mountains of Washington when going from 36 to 4 km grid spacing. Roberts et al. (2009) show that a substantial improvement in amount and spatial distribution of precipitation is obtained for a case in north-west England when the grid spacing is decreased from 12 km to 4 km, and further to 1 km. For heavy precipitation events in the Alps (including the extreme flooding in 2002) Kann and Haiden (2005) investigated the spatio-temporal scale-dependence of forecast skill for a model of given resolution (ALADIN, 10 km). They found large error reductions going from 100 to 1000 km<sup>2</sup> and from 1-h to 3-h accumulations.

With regard to the large-scale component of heavy precipitation events in the Alps, Schlemmer et al. (2010) point to the role of potential vorticity (PV) streamers associated with large-scale lifting and reduced static stability. The PV structure determines to what extent air is lifted rather than flowing around the Alps, which directly affects precipitation rates. For the event discussed here, Grams et al. (2014) analyse trajectories and demonstrate that quasi-stationary, continuous large-scale ascent in a north-south oriented warm conveyor belt was the key process causing high precipitation totals on the synoptic scale.

This paper is organized as follows. Section 2 provides a summary of the synoptic setting and observed precipitation distribution. Hydrological and atmospheric forecast performances during the event are analysed in Sections 3 and 4. In Section 5 the sensitivity of the precipitation forecasts with respect to model resolution, cloud microphysics, and soil moisture is investigated. A short summary and concluding remarks are given in Section 6.

## 2 Meteorological analysis

### 2.1 Synoptic setting

As is typical in such cases, this large-scale flood event was associated with a quasi-stationary upper-level low, leading to large precipitation accumulations in a specific area. On 28 May 2013 a pre-existing, negatively tilted trough over eastern Europe was reinforced by, and merged with, a trough which brought in stronger upper-level flow from the west. The merged system developed into a large cut-off low (Figure 1) which became quasi-stationary on 30 May 2013. Its centre remained located just east of the Alps until 2 June 2013. The centre of the associated surface low was located northeast of the Alps. As shown by Grams et al. (2014) using backward trajectories, moisture originating in northern Germany and Poland was carried towards the northern side of the Alps, where orographic lifting contributed substantially to the high observed precipitation totals. An important characteristic of this case was the ‘optimal’ (southward) direction of the moist, unstable airflow towards the west-east oriented alpine barrier, maximizing orographic lifting. Also, in the weeks leading up the event, rainfall totals were significantly above normal in large parts of central Europe. In Germany, for example, rainfall totals in May 2013 exceeded 200% of the 1961-1990 climatological average in a large swath reaching from the Baltic Sea to Bavaria (Stein et al., 2013).

The northerly airflow impinging on the Alps was very moist, with an overall lapse rate close to moist-adiabatic, and a low cloud base. Figure 2 shows the observed sounding in Munich at a time of intense

orographic precipitation in the Alps. Unsaturated layers which were present (between 500 and 600 hPa in the example shown) would have become saturated by a few 100 m of orographic lifting. Such an amount of lifting appears rather likely since significant flow deflection was restricted to below 850 hPa. As these drier layers also represent convectively unstable conditions, embedded convection may have played a role in the orographic precipitation enhancement.

Blöschl et al. (2013) compared the 2013 event with other severe flood cases (2002, 1954, 1899) in the Upper Danube basin and found that all four cases featured an extensive, quasi-stationary low over central/eastern Europe. There were some differences in the location of its centre, which was north/northeast of the Alps in 2013 and 2002, southeast in 1954, and east in 1899. However, orographic precipitation enhancement played an important role in all cases, and each time large precipitation accumulations were observed along the northern side of the Alps. In 2002 the highest amounts were actually observed further north (Elbe and northern Danube tributaries), but the orographic upslope precipitation belt formed a secondary maximum.

## 2.2 Precipitation and temperature

Two different operational analyses of the observed distribution of 72-h precipitation totals are shown in Figure 3. The top panel is the EFAS precipitation analysis, which is generated by interpolation of rain gauge observations, for the period 31 May 2013 06 UTC to 3 June 2013 06 UTC. The bottom panel is the precipitation analysis provided by the INCA system which interpolates between rain gauges using radar data and a parameterization of elevation effects (Haiden and Pistotnik, 2009; Haiden et al. 2011). Note that it shows the 72-h totals for the slightly earlier period 31 May 2013 00 UTC to 3 June 2013 00 UTC. The EFAS analysis is based on 24-h observations, and therefore only available for 06 UTC – 06 UTC. According to both analyses, precipitation totals exceeded 150 mm in a 300 km long belt along the northern alpine slopes. The INCA analysis also suggests that amounts exceeded 300 mm locally. Such high values are also suggested by the fact that the highest rain gauge value recorded in this event was 400 mm, recorded over a period of four days, at the station Aschau-Stein in Germany (Stein et al., 2013). The station is located at the entrance of a small, north-south oriented, funnel-shaped valley. It is likely that this particular topographic setting provided additional orographic precipitation enhancement at the local scale, superimposed on the broader orographic uplift at the alpine scale. At three stations close to the German/Austrian border the 4-day totals exceeded 300 mm according to Stein et al. (2013).

Heavy precipitation started to affect the northern parts of the Danube catchment on 29 May. In the northern alpine areas it started on 30 May, as the northerly airflow became established, and reached a first peak on 31 May (Figure 5). After a break of a few hours, precipitation rates increased again rapidly to reach maximum values around  $4 \text{ mm h}^{-1}$  (averaged over an area of  $\sim 30000 \text{ m}^2$ ) late on 1 June. During the course of 2 June rates decreased, but only slowly.

The large precipitation amounts occurred after an already very wet period in the weeks leading up to the flood, which exacerbated the hydrological response. With respect to temperature, the event was not the worst possible scenario, since the snowfall line was below 1500 m at first, moving up to only about 1800 m during the event (Blöschl et al. 2013). A significant fraction of northern alpine terrain is at a higher elevation, so the amount of water available for immediate runoff was noticeably reduced. It

would be worth investigating in a separate study the effect on discharge values of higher temperatures in order to represent a later time in the year (July-August) or the effect of global warming.

### 3 Meteorological forecast performance

#### 3.1 High-resolution forecast

The ECMWF high-resolution forecast (HRES) at T1279 (~16 km grid spacing) gave a very good indication of the area of maximum precipitation but generally underestimated amounts (Figure 4). Considering the limited spatial resolution of the model, and the fact that the precipitation in the worst affected area was heavily influenced by orographic effects, some underestimation is to be expected. However, there was also too little precipitation in the forecast for the western half of the Czech Republic, including its lower lying regions.

The lower panel in Figure 5 shows a sequence of forecasted cumulative precipitation forecasts for the northern alpine area as the event gets closer. Observations (black) show that the basic structure of the event was an initial 24-h precipitation period, followed by a 12-hour break, then by a 36-hour intense precipitation period. Forecasts start to show this pattern about 2 days before the beginning of the event. Most subsequent forecasts kept this structure, and the magnitude of the 72-h total increased from 80 to 110 mm. Allowing for an estimated uncertainty of the INCA analysis on the order of  $\pm 5\%$ , a conservative estimate of the under-prediction by the short-range forecast is 20-25%. A similar underestimation occurred in other models such as the UK Met Office global model and the National Center for Environmental Prediction (NCEP) global GFS model (not shown), whereas limited area models such as ALARO and AROME came much closer to observations (Yan et al., 2014).

#### 3.2 Ensemble forecast

We first evaluate the performance of the ECMWF ensemble control forecast (CTRL) in the same way as the HRES. Comparison of Figures 5 and 6 shows that the CTRL is very similar to the HRES. The difference in resolution between the two runs (32 vs 16 km) produces only a small difference in total precipitation amounts in this case. Figure 7 shows that at forecast day 5 there is considerable spread with about 80% of members indicating amounts between 10 and 40 mm, and 20% between 40 and 100 mm. The double-peaked character (in terms of intensity) of the event is not yet captured by the forecast. At forecast day 2 the total spread has not decreased much, but the range of 40-80 mm has become much more likely, and the lower limit has increased to almost 30 mm. There is also an indication that the event will consist of two more intense periods separated by a 'break'.

At forecast day 0 the spread has become considerably smaller, spanning the range from 60 to 100 mm. At this lead time predictability effects are relatively smaller, and the systematic underestimation seen in the HRES and CTRL becomes apparent. It is interesting to note that the first intense period up to about 24 h is rather well captured in terms of magnitude, whereas the second, more intense one, is not. To see whether this problem persisted in later forecasts, we take a look at the ENS initialized 24 hours into the event (lower right panel in Figure 7). As expected, the spread has become smaller still, and final amounts at 72 h are now 20 mm higher (10 mm due to the matching with observations at 24 h, and 10 mm due to an actual increase in the forecasted amounts) but the general underestimation is still present.

The Extreme Forecast Index (EFI) is an ECMWF product for severe weather (Zsoter, 2006) which shows how anomalous a given forecast is compared to the model climate. At the time of the forecast the model climate was obtained by running a re-forecast suite of 5 ensemble members for the past 20 years. The shift of tails (SOT) has been designed to complement the EFI by providing additional information about the magnitude of an event, showing how extreme the tail of a given ensemble forecast distribution is compared to the tail of the model climate distribution. In this case the EFI gave a strong signal of anomalously wet conditions over Central and south-east Europe more than 10 days in advance (Figure 8). SOT suggested the possibility of an exceptionally extreme event since its values indicated that at least 10% of the 51 ensemble members forecast 5-day rainfall accumulations higher than the 99th model climate quantile (Figure 8). Closer to the event the EFI signal became stronger and increasingly focused with respect to location, providing growing confidence in the prediction that an extreme event will occur.

It should be noted that the ECMWF forecasts, although underestimating the magnitude of the event in absolute terms, indicated an exceptional event relative to the model climate. Compared to the model climate the predicted amounts were well above the extremes obtained from running a re-forecast suite over the past 20 years. This is illustrated in Figure 9 which shows cumulative distributions of forecasts for the station Mattsee (near the city of Salzburg, Austria), where 195 mm were observed in 72 h, along with the model climate (thick black line). Especially at shorter lead times the majority of ensemble members exceeded the 99th percentile of the model climate distribution. In this relative sense the model captured the exceptional magnitude of the event (Figure 9).

## 4 Hydrological forecast performance

Streamflow forecasts from the European Flood Awareness system (EFAS, Thielen et al., 2009; Bartholmes et al., 2009) to a large extent confirmed the results from the meteorological analysis that the location of the most affected areas was generally well forecast but the magnitude was underestimated.

EFAS flood *alerts* are issued when the probability of exceeding critical flood thresholds are forecasted more than 2 days ahead in a river basin which is covered by an EFAS partner and has a minimum upstream area of more than 4000 km<sup>2</sup>. EFAS flood *watches* are issued when a certain probability of exceeding critical flood thresholds is forecasted in a river basin for which an EFAS partner exists but the forecasted event does not satisfy the rules of an EFAS alert, for example regarding warning lead time, size of river basin, or location of event. An EFAS flood watch can also be issued if EFAS results are not conclusive but one of the multiple forecasts indicates risk of severe flooding.

Over the last week of May, EFAS forecasts showed a rapidly increasing probability of exceeding flood warning thresholds for wide areas in Central Europe including Germany, Poland, Austria, Czech Republic and Slovakia. Between 28 and 31 May, 14 EFAS flood warnings of different severity levels (both flood alerts and watches) were issued for some of the major rivers (e.g. Elbe, Danube, Rhine and Odra) up to 8 days before the beginning of the extreme streamflow conditions (Figure 10). Cities such as Wittenberg (Germany) were severely affected by the rising waters of the Elbe, where the record high of the ‘flood of the century’ in the year 2002 was surpassed by more than half a metre on 9 June 2013.

EFAS also provides flash flood warnings based on the European Precipitation Index (EPIC, Alfieri and Thielen, 2012). In consecutive forecast runs it picked up the extreme character of the upcoming precipitation event over a large area centred along the Austrian-German border, indicating high probability of flash flooding in a number of alpine catchments (Figure 11). An EFAS watch for extreme precipitation and possible flash flooding was issued for this area on 1 June, with 30-36 hours lead time on the event peak. This area was indeed severely affected by extreme weather on 1 and 2 June. The city of Passau in southern Germany was particularly badly hit, with water levels reaching their highest value for the past 500 years.

The verification scores over Europe for the whole event confirm the analysis of the meteorological forecasts. There were robust indications of an extreme event, but the actual intensity was underestimated. Figure 12 shows that the mean error of the streamflow on forecast day 7, expressed here as a percentage relative to the mean observed value, shows a clear underestimation in the most affected area.

## 5 Sensitivity studies

### 5.1 Horizontal resolution

As described in Section 2, the flow was mainly northerly during the period 31 May to 3 June, and maximum precipitation accumulations were observed along the northern slopes of the Alps, indicating strong orographic effects. Upslope precipitation enhancement is closely related to the steepness of the terrain and therefore sensitive to model resolution. In order to investigate the impact of model resolution on the forecast we compare model runs made with T319 (64 km), T639 (32 km), T1279 (16 km), and T2047 (10 km), all with the most recent model cycle 40r1, which became operational in Nov 2013, after the event. Forecasts are run for 5 different initial times 12 hours apart, from 29 May 00 UTC to 31 May 00 UTC. Figure 13 shows the mean precipitation inside the box 47-48 N, 10-14 W accumulated over the 72-h period 31 May 06 UTC to 3 June 06 UTC. The value for this area estimated from interpolation of raingauge observations (EFAS) is 120 mm, the value obtained from the INCA analysis system (raingauge + radar + parameterization of orographic effects) is 148 mm. The x-axis represents the initial time of the forecasts. For the last three forecasts, T2047 produces the highest precipitation inside the box, but never exceeds 110 mm and therefore still falls short of the likely range of observed values.

Changing the model resolution alters not just the magnitude of orographic precipitation enhancement but the entire evolution of the atmospheric state. Precipitation totals shown in Figure 13 are therefore not necessarily ranked according to model resolution. However, at the lead time when the forecasts give the highest precipitation, and thus are closest to observations (30 May 12 UTC), they are ranked according to resolution. This suggests that at this particular initialization time the resolution-dependent orographic upslope effect accounts for a large part of the differences. The corresponding spatial distribution of precipitation for the four different resolutions (all initialized at 30 May 12 UTC) is shown in Figure 14. While the large-scale features of the precipitation field do not differ dramatically between the runs, the amount of orographic enhancement in the alpine area can be seen to increase with increasing resolution. The precipitation distribution in the Czech Republic is also sensitive to resolution, with the higher resolution runs producing a much more pronounced west-east gradient.

This is not directly connected to orographic uplift, as this gradient is perpendicular to the main mountain ranges in the area.

For steady-state, saturated flow towards a mountain barrier the orographic precipitation enhancement is to first order proportional to the product of wind speed and terrain slope. In order to diagnose the effect of different wind speeds perpendicular to the Alps in the different forecasts, Figure 15 shows forecasted areal precipitation amounts (T1279) in the previously defined box (47-48 N, 10-14 W) as a function of the meridional wind component at 700 hPa, averaged over 48-49 N, 10-14 W (just to the north of the precipitation box) for the period 31 May 06 UTC to 3 June 06 UTC. The mean northerly flow for the period in the analysis was  $10.5 \text{ m s}^{-1}$ , corresponding to a fetch of about 2700 km. As expected there is a relationship between the northerly flow and the precipitation amount, and for a given wind speed the higher resolution runs generally give more precipitation. Despite the limited number of data points, the two highest resolutions appear to have a stronger wind-precipitation relationship than the two lowest resolutions.

Figure 16 shows the same as Figure 15 but for each member of all ensemble forecasts initialized between 26 June and 31 June, giving 500 individual forecasts (T639) in total. A well-defined, slightly non-linear relationship between northerly flow and precipitation is apparent, but none of the members gets close to the observed values of 140-150 mm, even though the predicted wind speeds reach, and even exceed, the analysed value of  $10.5 \text{ m s}^{-1}$ .

While the horizontal resolution upgrade of the ECMWF operational HRES planned for 2015 will be a move to 10 km, experimentation has already started with a still higher resolution of T3999 (5 km). Current computer resources do not yet allow a general evaluation of forecasts at this resolution. However, it is of interest to investigate the impact on severe weather events, as has been done for hurricane Sandy (Magnusson et al., 2014). For this flood case, T3999 simulations were performed for the initialization time of 30 May 12 UTC, when the areal distribution was generally well predicted by the lower resolution runs and the operational run. At a resolution of 5 km the model is in the so called 'grey zone' where the relationship between parameterized deep convection and explicit deep convection on the grid scale becomes less clear. Figure 17 therefore shows both results with parameterized convection (left) and without parameterized convection (right). Especially in the run with deep convection the precipitation rates are clearly improved, with a 72-h precipitation accumulation inside the alpine box of 128 mm compared to 109 mm in the operational forecast (Figure 18).

A comparison of cumulative precipitation amounts inside the alpine box from the different resolution runs (all initialized at 30 May 12 UTC and using the model physics of 40r1) is shown in Figure 18. The largest increase of precipitation occurs between the two lowest resolutions. It can be seen that future upgrades beyond the currently operational T1279 can be expected to give an additional benefit in situations like this.

## 5.2 Cloud microphysics

Another possible cause of the underestimation of orographic precipitation enhancement in the operational forecast in this case is the cloud microphysical parameterization, specifically the conversion from cloud water species (liquid and ice) to precipitation. The ECMWF model uses a formulation proposed by Sundqvist et al. (1978) which combines the processes of autoconversion and

accretion into one term (SQ scheme). This makes it more difficult to properly describe the different characteristics of precipitation formation in weak (drizzle) and strong cases. A new formulation (KK scheme) based on results from drop-spectrum resolving simulations (Khairoutdinov and Kogan, 2000) will be implemented in the operational model in 2014. It parameterizes autoconversion and accretion by two separate terms and allows a more nonlinear representation of precipitation formation. It has been tested on the case studied here, and results are shown in Figure 19 for model runs at T1279 and T3999 initialized at 30 May 12 UTC, which is the same initialization time as for the resolution sensitivity runs.

Accumulated over the 72-h period, the KK scheme gives about 10% more precipitation than the SQ scheme at the operational model resolution (T1279). It slightly decreases precipitation in the first 18 h of the event and increases it in the last 36 h, thereby bringing forecasts closer to observations in both sub-periods. Applying the same scheme at T3999 gives a slightly smaller increase, however the combination of high resolution and KK scheme brings the total amount still closer to observations.

Two additional experiments (SQ1000) at T3999 were performed with deep convection switched on and off, in which the autoconversion time-scale of the Sundqvist scheme was reduced from 6000 to 1000 s (see also Figure 17, bottom panels). This is a value suggested by cloud-resolving models, and more appropriate at a resolution of 5 km. With this setting the resulting precipitation field becomes even closer to observations, not just in the alpine area, but also in the Czech Republic. The total amount in the alpine box reaches 135 mm and 144 mm (Figure 19). It is interesting that the high-resolution runs generally produce a better areal distribution in the Czech Republic, with the heavy precipitation extending further east. Analyses based on high-density observations provided by Brozkova et al. (2013) show a band of heavy precipitation oriented NE-SW which extends through the whole country. Its shape and location are very similar to that seen in the run with enhanced autoconversion.

The experiment with enhanced autoconversion and the deep convection scheme switched on is very close to observations, and within the likely range of the INCA analysis uncertainty ( $\pm 5\%$ ). Although such a model configuration does not appear tenable globally (leading to widespread overestimation of precipitation) it highlights the sensitivity of extreme orographic precipitation to parameterization choices.

### 5.3 Soil moisture

Reliable forecasts of such extreme flood events require good representation of the degree of soil moisture saturation. In this Section the soil moisture conditions of the ECMWF forecasting system are assessed for the period from 29 May to 03 June 2013, just before the peak flood occurred. Figure 20 shows the ECMWF operational mean soil moisture anomaly in the root zone (first metre of soil) from 29 May to 03 June 2013 compared to the mean of the same 6-day period averaged over the years 2008 to 2012. The figure shows a wet anomaly for most of Europe in 2013 compared to the same period in 2008-2012, with values ranging between 100 mm and 150 mm of water in central Europe, and local anomalies reaching values larger than 150 mm.

To address the effect of soil moisture initialisation on the saturation level of soil moisture in such extremely wet conditions, a set of four data assimilation experiments were conducted with the IFS at 25 km resolution from 01 May 2013 to 15 June 2013. Firstly, an Open Loop experiment was set-up in

which the soil moisture data assimilation was deactivated; in this experiment the soil moisture dynamics is entirely controlled by the land surface model H-TESEL (Balsamo et al., 2009; Albergel et al., 2012), however it benefits from the atmospheric and soil temperature data assimilation which were kept active. Secondly, an Extended Kalman Filter (EKF) experiment was conducted with the soil moisture initialisation relying on the use of screen level observations, as used in operations at ECMWF (de Rosnay et al., 2013). Finally, two experiments were conducted using satellite soil moisture observations from the Advanced Scatterometer (ASCAT) (de Rosnay et al., 2014), and brightness temperature observations from the Soil Moisture and Ocean Salinity (SMOS) dataset (Muñoz Sabater et al., 2012). The four experiments are consistent in terms of soil moisture patterns and location of maximum soil moisture values (not shown). Table 1 shows mean soil moisture values obtained for these experiments from 29 May to 03 June 2013 in an area of 2 degrees by 2 degrees (48N-50N, 8E-10E) where maximum surface soil moisture values were consistently obtained in all experiments. For reference, the model saturation and field capacity values, which result from the soil texture information used in the land surface model for this area, are also indicated. The table clearly shows that all experiments reproduce mean soil moisture values ranging from 42.4 % (percent by volume) to 43.2 %, well above the field capacity (36.4 %) and very close to the saturation level (44.8 %). Generated runoff was compared and it was also found to be very similar for the four experiments (not shown).

*Table 1: Sensitivity of surface mean soil moisture to soil moisture initialisation method from 29 May to 03 June 2013 for the area of maximum soil moisture values (48N-50N, 8E-10E). Results are shown for an Open Loop (OL) experiment, i.e. without soil moisture data assimilation, an EKF soil moisture analysis relying only on screen level data assimilation (as used in operations at ECMWF), and for combining screen level observations with ASCAT or SMOS satellite observations. The last two columns show the model theoretical saturated and field capacity soil moisture values for this area.*

	<b>OL no assimilation</b>	<b>EKF as in operation</b>	<b>EKF and ASCAT</b>	<b>EKF and SMOS</b>	<b>Saturated value</b>	<b>Field capacity</b>
<b>Soil moisture (% m<sup>3</sup>m<sup>-3</sup>)</b>	43.2	43.1	43.1	42.4	44.8	36.4

The results of these sensitivity experiments indicate that the saturated soil conditions prior and during the event were well represented by the soil moisture data assimilation experiments and in the open loop model. The experiments suggest that in this case the different observation types used to analyse soil moisture did not bring additional useful information to an already saturated soil in the open loop model. Hence, the soil moisture initialisation approach had negligible influence on the soil moisture saturation degree. Representing saturated soil moisture conditions is a necessary condition to ensure the flood forecast is accurate. It is however not a sufficient condition since subsequent flooding is rather directly controlled by precipitation amounts as shown in Sections 4 and 5.4.

## 5.4 Impacts on Hydrology

The experiments with different resolutions and physics as described in Sections 5.1 and 5.2 were subsequently run through the EFAS system in an offline version which has the same setup as the current operational version. In operational hydrological forecasts, the initial conditions are usually

given by running the hydrological model with observed precipitation and temperature as close to the initial time as possible, then filling up the gap (typically 12 hours) with the latest operational NWP (due to the time lag until observations are received). The run for the initial conditions is called the water-balance run, and represents a forecast with a 'perfect' atmosphere, indicating the potential predictability of the hydrological forecast. As in the meteorological sensitivity studies, the hydrological forecast from 30 May 12 UTC is considered.

The simulated runoff by the EFAS system from experiments with different resolutions in general follows the results of the precipitation pattern when analysed over the alpine box (not shown). This is to be expected since the precipitation is the driving force. The runoff response to a precipitation event is not always linear, but in this case the soil was saturated and almost all of the rainfall resulted in runoff.

In a hydrological model, the runoff is routed through stream channels to model discharge, and here the timing is as important as the magnitude of the precipitation. An example of this is seen in Figure 21, where the simulated discharge in the town of Passau at the German/Austrian border is compared for different model resolutions. The black line is the modelled discharge with observed precipitation. Passau is on the headwaters of the Danube, and it is located at the confluence of the Inn and Danube rivers. The town of Passau was severely hit by flooding, and the observed peak discharge was estimated as high as 10000 m<sup>3</sup>/s, which is beyond the range of what the EFAS system currently can predict; the hydrological model with observed precipitation gave 6000 m<sup>3</sup>/s. The simulations with precipitation from the different atmospheric experiments gave on the order of 4000 m<sup>3</sup>/s. The ordering of the experiments follows what was seen for precipitation, with the highest values for the highest resolution (T3999: 4500 m<sup>3</sup>/s).

Figure 22 shows the impact of improved cloud physics for the generation of precipitation, both for the current model version and for the T3999 model. The improvement in discharge at this critical location is substantial, although levels in the forecasts are still below the potential level of skill of the hydrological forecast (black line). For this event, an error in location of precipitation can lead to large errors in the magnitude of the discharge, if the runoff appears in another basin. For the alpine region as a whole, the improvements in model resolution as well as physics greatly reduced the underestimation of precipitation. This particular location was chosen to highlight that even with a well performing hydro-meteorological forecasting system it is still difficult to predict peak discharges for extreme events like the one experienced in June 2013.

## 6 Conclusions

In this report the performance of the IFS and the EFAS during the June 2013 flooding in Central Europe have been investigated. This was a severe, large-scale event which affected several countries and led to the loss of life as well as considerable damage in two major European catchments (Danube, Elbe). The large-scale synoptic setting was typical of events of this type, with a slow-moving upper level low, and a continuous stream of relatively warm, moist low-level air towards the northern side of the Alps. Orographic lifting in the Alps and along mountain ranges in the Czech Republic and Germany caused significant precipitation enhancement.

The IFS precipitation forecasts were generally satisfactory with respect to the location of the area of the heaviest precipitation (south-eastern Germany, Austria) but even at the short range underestimated the magnitude by at least 25% over the northern Alps. As a consequence, EFAS streamflow forecasts using IFS data as input underestimated the peak discharges for the Danube. Predictions for the Elbe, where orographic enhancement did not play as dominant a role as for the Danube, were reasonable.

Forecasts of precipitation amounts in the alpine areas did not increase with resolution at all lead times. However, runs initialized on 30 May 12 UTC (one day before the onset of the event) gave forecasted amounts closest to observations and produced precipitation totals ranked according to resolution. This was most pronounced for the difference between T319 (64 km) and T639 (32 km), and also for the change from the currently operational T1279 (16 km) to T2047 (10 km), providing a preview for the next resolution upgrade of the IFS. We also made simulations at still higher resolution (T3999, 5 km) which gave an additional increase in precipitation. Interestingly, increasing the resolution also appeared to improve the forecast of a non-orographic band of precipitation across the Czech Republic. This improvement was more pronounced when the autoconversion rate in the Sunqvist microphysics parameterization was increased to a value more suitable for the higher model resolution. This experiment provided a value for the northern Alps close to the estimate from the INCA analysis.

Encouraging results were also obtained by using a new formulation for the autoconversion and accretion processes which is planned to be introduced operationally in 2014. For this event it gives an increase of the total rainfall amount in the alpine upslope area of about 10%. It also captures the difference in intensity between the first and the second parts of the event somewhat better than the operational scheme.

Soil moisture, which is an important factor due to its effects both on surface evaporation and runoff, was found to be well simulated by the IFS. The (near-)saturated conditions during this event were well captured in the ‘open-loop’ configuration where no assimilation of soil moisture is performed and the model evolves the water content of the soil solely based on its own budget computations.

Finally, the different atmospheric experiments were used as forcing for the hydrological model. As a benchmark for the forecasts, the system was also forced by observed precipitation to obtain the water discharge with a perfect atmospheric model. For Passau, situated in southern Germany at a critical location along the Danube, this simulation still underestimated the peak flow. With the atmospheric forecast the streamflow was further reduced due to underestimated precipitation, but the simulation with the highest resolution and improved physics clearly improved the flow predictions.

The findings in this study suggest that the underestimation of precipitation in the operational forecast at short range was partly due to the current resolution of the model. Another substantial contribution can be attributed to the formulation of autoconversion and accretion, which will be updated in 2014. It has been shown that these improvements would benefit the hydrological forecast as well, although the extremely high (500-year) peak discharge in Passau at the confluence of Inn and Danube remains a challenge. In general, for extreme events such as this one it is important that hydrological forecasts are driven by meteorological ensemble forecasts, since extreme precipitation amounts in the right areas may be present only in some of the members.

The very strong orographic precipitation enhancement observed during this event, as well as the availability of high-resolution analyses by the INCA system, makes it a useful test case for resolution

upgrades and microphysics changes. While not too much weight can be put on a single case it could provide part of a set of extreme events to be simulated with a new model version before it becomes an e-suite.

## Acknowledgements

We would like to thank the Central Institute for Meteorology and Geodynamics (ZAMG) in Vienna for providing INCA precipitation analysis data.

## References

- Albergel C., G. Balsamo, P. de Rosnay P., J. Muñoz-Sabater, and S. Boussetta, 2012: A bare ground evaporation revision in the ECMWF land-surface scheme: evaluation of its impact using ground soil moisture and satellite microwave data. *Hydrol. Earth Syst. Sci.*, **16**, 3607-3620.
- Alfieri, L. and J. Thielen, 2012: A European precipitation index for extreme rain-storm and flash flood early warning. *Meteorol. Appl.*, DOI: 10.1002/met.1328.
- Balsamo G., P. Viterbo, A. Beljaars, B. van den Hurk, M. Hirschi, A.K. Betts, K. Scipal, 2009: A revised hydrology for the ECMWF model: Verification from field site to terrestrial water storage and impact in the Integrated Forecast System. *J. Hydrol.*, **10**, 623–643.
- Bartholmes, J. C., J. Thielen, M. H. Ramos, and S. Gentilini, 2009: The European Flood Alert System EFAS - Part 2: Statistical skill assessment of probabilistic and deterministic operational forecasts. *Hydrol. Earth Syst. Sci.*, **13**, 141-153.
- Blöschl, G., T. Nester, J. Komma, J. Parajka, and R. A. P. Perdigao, 2013: The June 2013 flood in the Upper Danube basin, and comparisons with the 2002, 1954, and 1899 floods. *Hydrol. Earth Syst. Sci.*, **17**, 5197-5212.
- Brozkova, R., M. Sandev, and J. Masek, 2013: QPF Forecast by the IFS model during the flood episodes in June 2013 – discussion of some results. CHMI report, 18p.
- Dee, D. P., S. M. Uppala, A. J. Simmons, P. Berrisford, P. Poli, S. Kobayashi, U. Andrae et al., 2011: The ERA-Interim Reanalysis: Configuration and Performance of the Data Assimilation System. *Q. J. R. Meteorol. Soc.*, **137**, 553–597.
- de Rosnay P., M. Drusch, D. Vasiljevic, G. Balsamo, C. Albergel and L. Isaksen, 2013: A simplified Extended Kalman Filter for the global operational soil moisture analysis at ECMWF. *Q. J. R. Meteorol. Soc.*, **139**, 1199-1213.
- de Rosnay P., G. Balsamo, C. Albergel J. Muñoz-Sabater and L. Isaksen, 2014: Initialisation of land surface variables for Numerical Weather Prediction. *Surveys in Geophysics*, **35**, 607-621.
- Grams, C. M., H. Binder, S. Pfahl, N. Piaget, and H. Wernli, 2014: Atmospheric processes triggering the Central European floods in June 2013. *Nat. Hazards Earth Syst. Sci. Discuss.*, **2**, 427-258.
- Haiden, T., and G. Pistotnik, 2009: Intensity-dependent parameterization of elevation effects in precipitation analysis. *Adv. Geosci.*, **20**, 33-38.

- Haiden, T., A. Kann, C. Wittmann, G. Pistotnik, B. Bica, and C. Gruber, 2011: The Integrated Nowcasting through Comprehensive Analysis (INCA) system and its validation over the Eastern Alpine region. *Wea. Forecasting*, **26**, 166-183.
- Kann, A., and T. Haiden, 2005: The August 2002 flood in Austria: sensitivity of precipitation forecast skill to area size and duration. *Meteorol. Z.*, **14**, 369-377.
- Khairoutdinov, M., and Y. Kogan, 2000: A new cloud physics parameterization in a large-eddy simulation model of marine stratocumulus. *Mon. Wea. Rev.*, **128**, 229-243.
- Magnusson, L., J.-R. Bidlot, S. Lang, A. Thorpe, N. Wedi, and M. Yamaguchi, 2014: Evaluation of medium-range forecasts for hurricane Sandy. *Mon. Wea. Rev.*, **142**, (in press).
- Muñoz Sabater J., A. Fouilloux and P. de Rosnay, 2012: Technical implementation of SMOS data in the ECMWF Integrated Forecasting System. *Geosci. Remote Sens. Let.*, **9**, 252-256.
- Richardson, D. S., J. Bidlot, L. Ferranti, T. Haiden, T. Hewson, M. Janousek, F. Prates, and F. Vitart, 2013: Evaluation of ECMWF forecasts, including 2012–2013 upgrades. *ECMWF Technical Memorandum*, No. 710, ECMWF, Reading, United Kingdom, 54p.
- Roberts, N. M., S. J. Cole, R. M. Forbes, R. J. Moore, and D. Boswell, 2009: Use of high-resolution NWP rainfall and river flow forecasts for advance warning of the Carlisle flood, north-west England. *Meteorol. Appl.*, **16**, 23-34.
- Schlemmer, L., O. Martius, M. Sprenger, C. Schwierz, and A. Twitchett, 2010: Disentangling the forcing mechanisms of a heavy precipitation event along the alpine south side using potential vorticity inversion. *Mon. Wea. Rev.*, **138**, 2336-2353.
- Stein, C., G. Malitz, and Co-authors, 2013: Das Hochwasser an Elbe und Donau im Juni 2013. *Berichte des Deutschen Wetterdienstes*, No 242, 36p.
- Sundqvist, H., 1978: A parameterization scheme for non-convective condensation including prediction of cloud water content. *Quart. J. Roy. Meteor. Soc.*, **104**, 677-690.
- Thielen-del Pozo, J., J. Bartholmes, M.-H. Ramos, A. de Roo, 2009: The European Flood Alert System. Part 1: Concept and development. *Hydrol. Earth Syst. Sci.*, **13**, 125-140.
- Westrick, K. J., and C. F. Mass, 2001: An evaluation of a high-resolution hydrometeorological forecast system for prediction of a cool-season flood event in a coastal mountainous watershed. *J. Hydromet.*, **2**, 161-180.
- Wilks, D. S., 2006: *Statistical Methods in the Atmospheric Sciences*. 2nd ed. International Geophysics Series, Vol. 59, Academic Press, 629p.
- Wittmann, C., Haiden, T., and A. Kann, 2010: Evaluating multi-scale precipitation forecasts using high resolution analysis. *Adv. Sci. Res.*, **4**, 89-98.
- Yan, X., C. Wittmann, and F. Meier, 2014: AROME in Austria. ALADIN-HIRLAM Newsletter No. 2, 27-32.
- Zsoter, E., 2006: Recent developments in extreme weather forecasting. *ECMWF Newsletter*, No. 107, ECMWF, Reading, United Kingdom, 8-17.

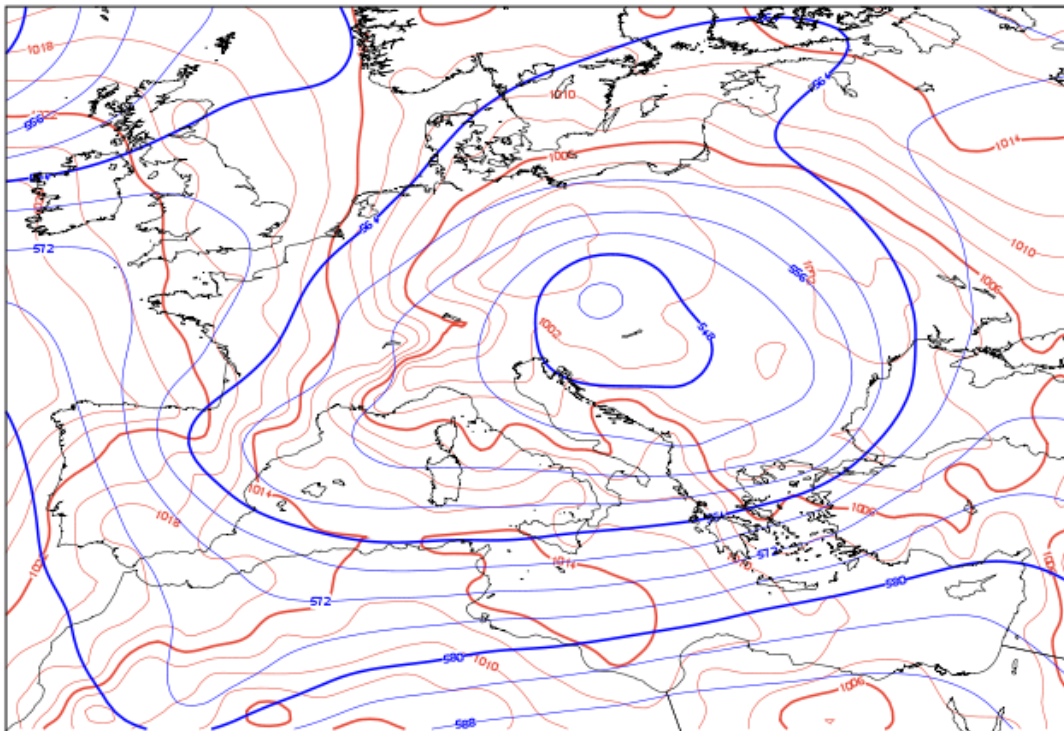


*Figure 1. Analysis of 500 hPa geopotential (blue) and mean sea level pressure (red) on 31 May 2013 at 12 UTC.*

02/06/2013 00UTC; WMO id: 10868

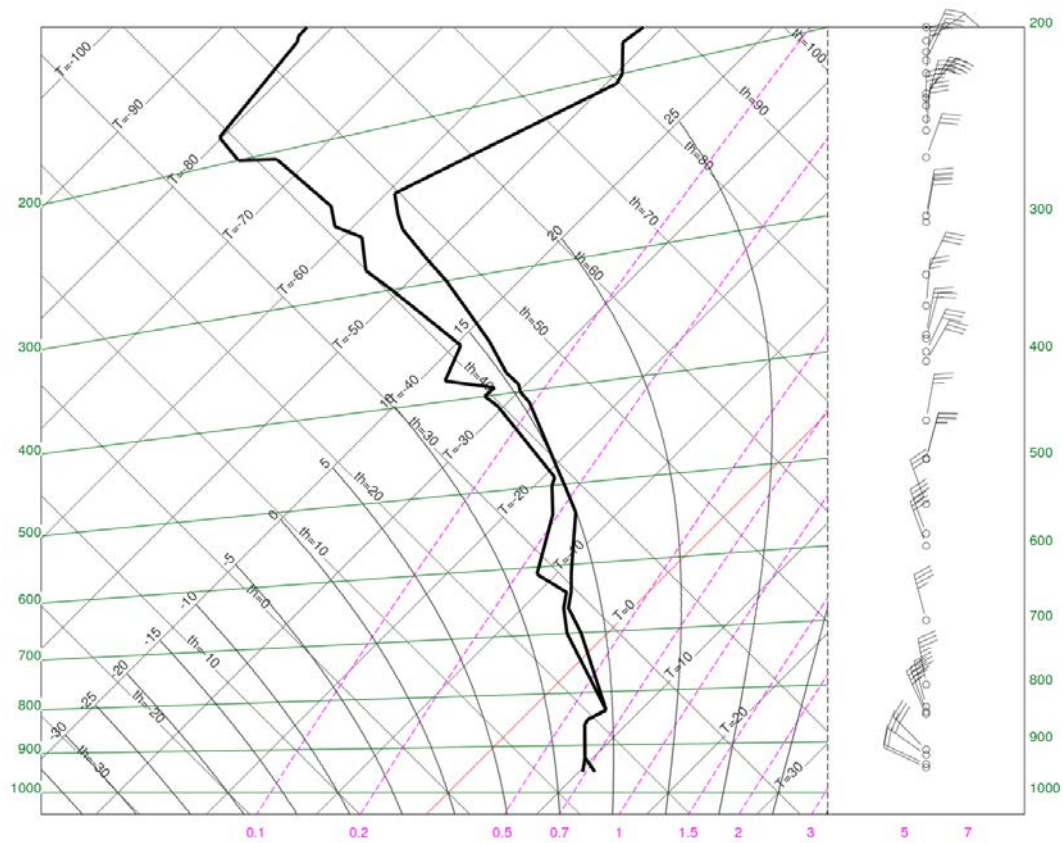


Figure 2. Upstream sounding at Munich on 2 June 2013 at 00 UTC, during the period of most intense orographic precipitation.

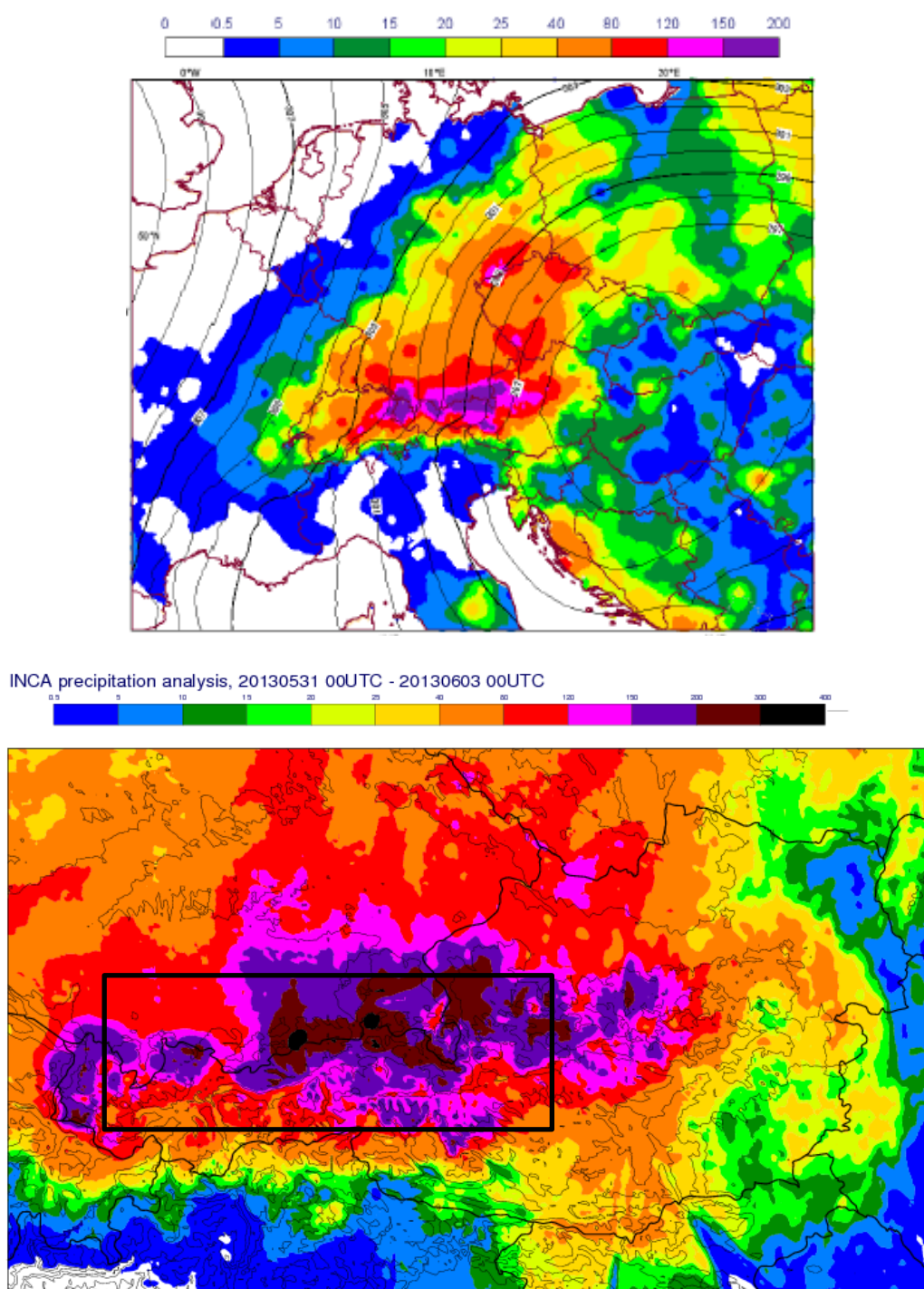


Figure 3. (a) EFAS precipitation analysis for the period 2013-05-31 06 UTC - 2013-06-03 06 UTC based on raingauge data. Isolines in the upper panel show 700 hPa geopotential from the ECMWF analysis, averaged over the same period; (b) INCA analysis for the period 2013-05-31 00 UTC - 2013-06-03 00 UTC based on radar and raingauge data. Isolines show INCA 1 km topography. The rectangle indicates the averaging area 47-48 N, 10-14 E referred to in subsequent plots.

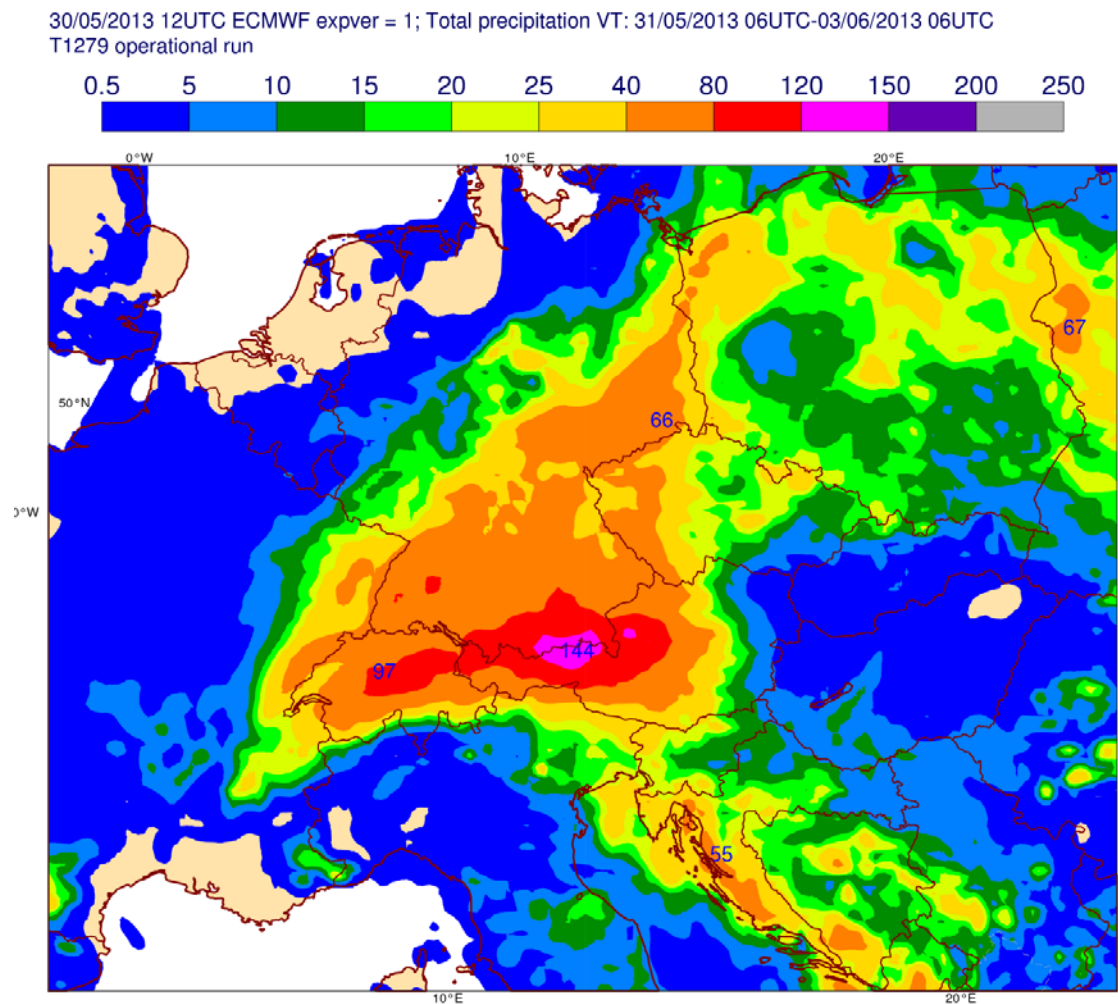


Figure 4. ECMWF operational high-resolution forecast of 72-h precipitation totals from 2013-05-31 06 UTC to 2013-06-03 06 UTC, initialized at 2013-05-30 12 UTC.

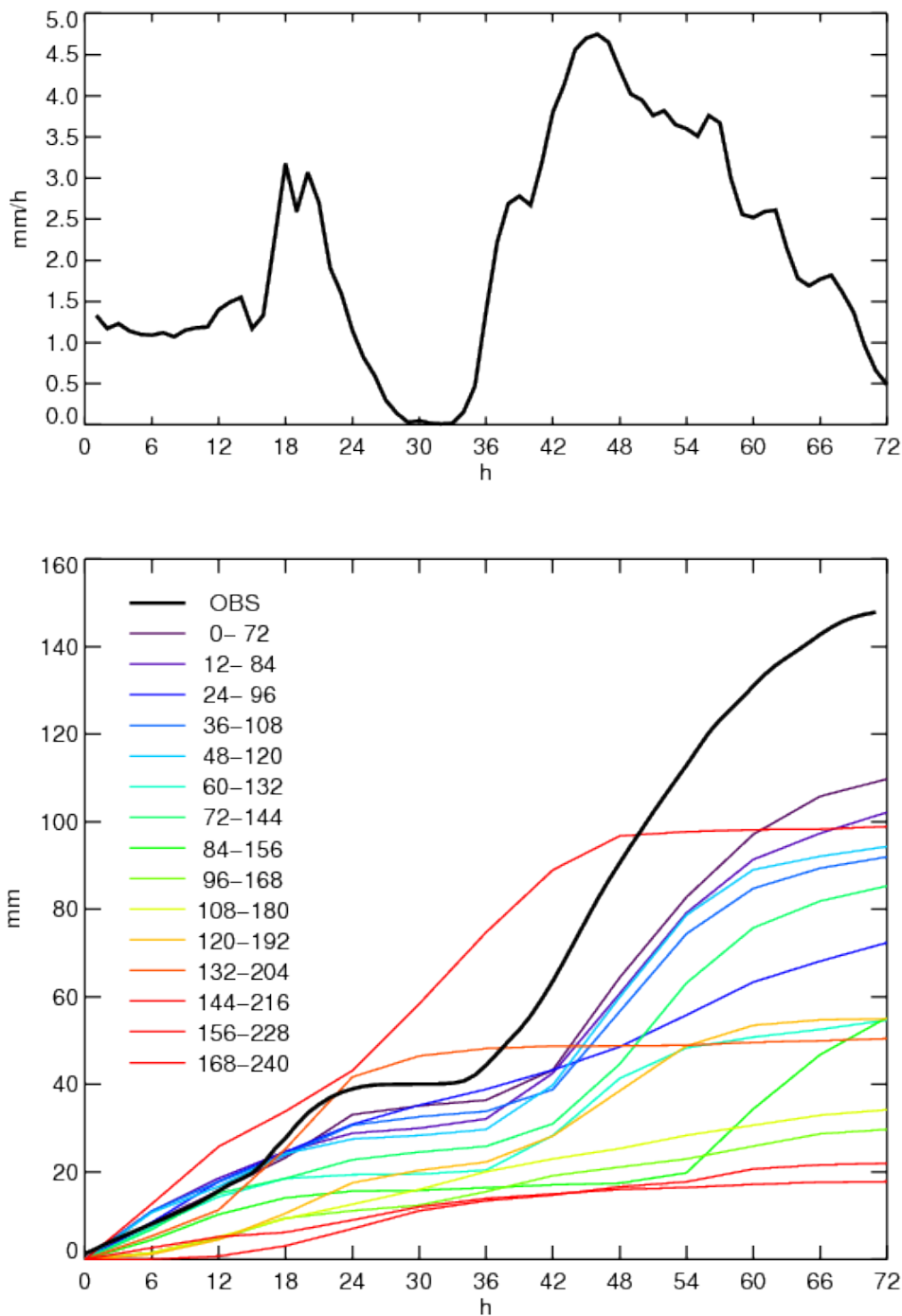


Figure 5. Precipitation intensity (1-hourly, top) and cumulative precipitation (bottom) in the area 47-48 N, 10-14 E (shown in Figure 3), computed from operational 15-min INCA analyses. The lower panel also shows ECMWF high-resolution cumulative precipitation forecasts for different lead times. The accumulation begins at 31 May 2013 00 UTC.

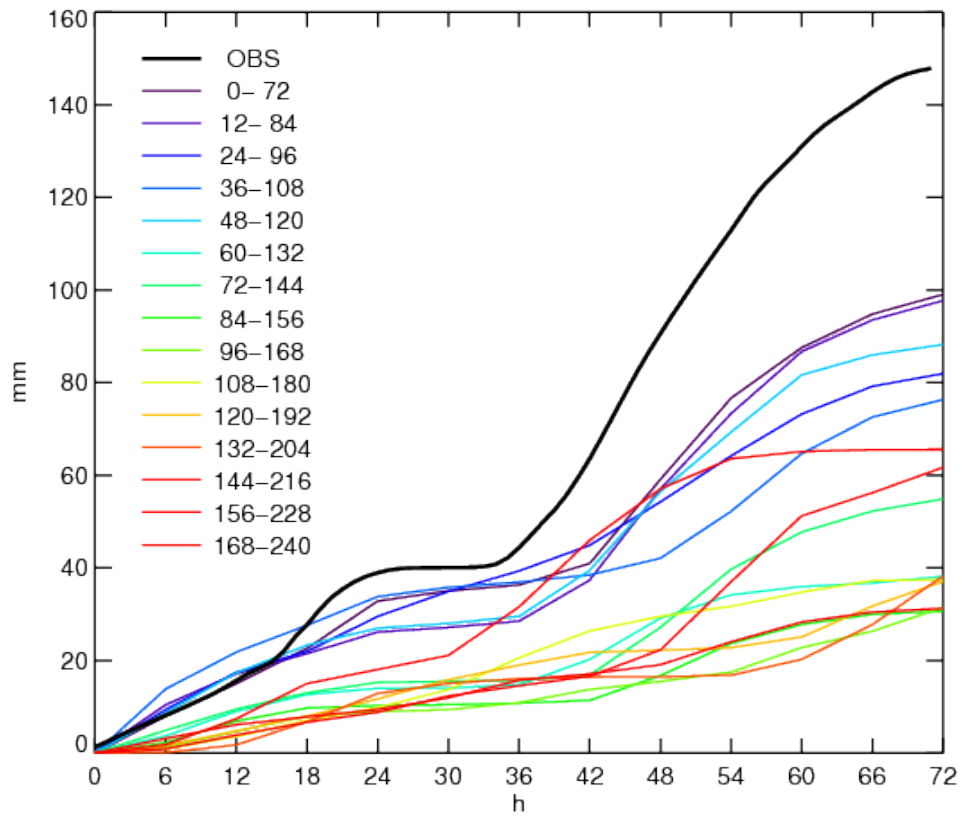


Figure 6. Same as the lower panel of Figure 5 but for CTRL instead of HRES.

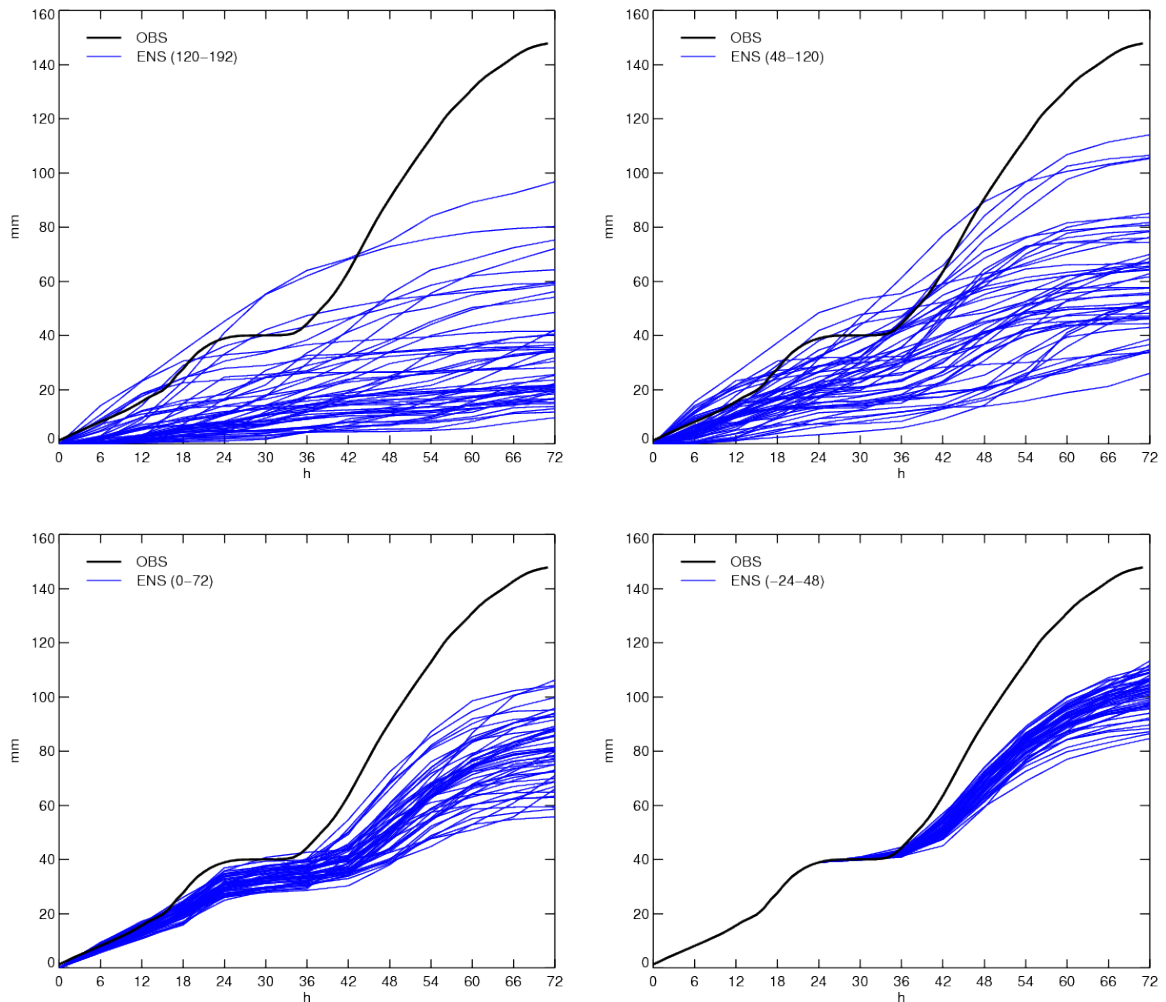


Figure 7. Cumulative precipitation from the 50 individual members of the ECMWF ensemble forecast in the area 47-48 N, 10-14 E for lead times of 120, 48, 0, and -24 hours relative to the beginning of the event (31 May 2013 00 UTC).

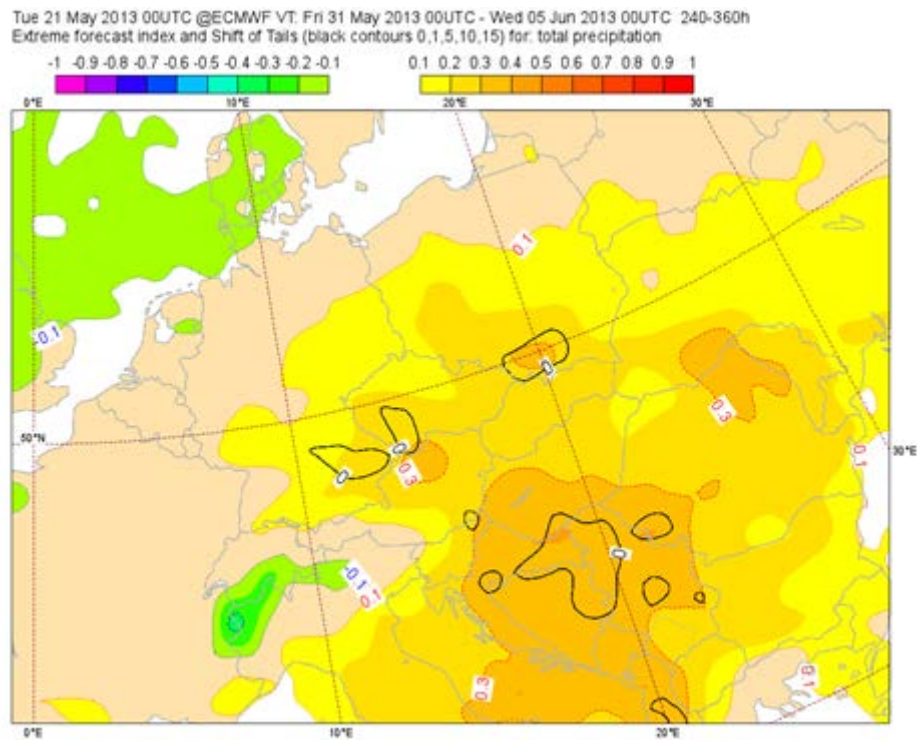


Figure 8. EFI (shaded) and SOT (black contours) from 21 May 2013 00 UTC for T+240-360h valid from 31 May 2013 00 UTC to 5 June 2013 00UTC. Positive EFI and SOT indicate an increased risk of anomalously wet conditions.

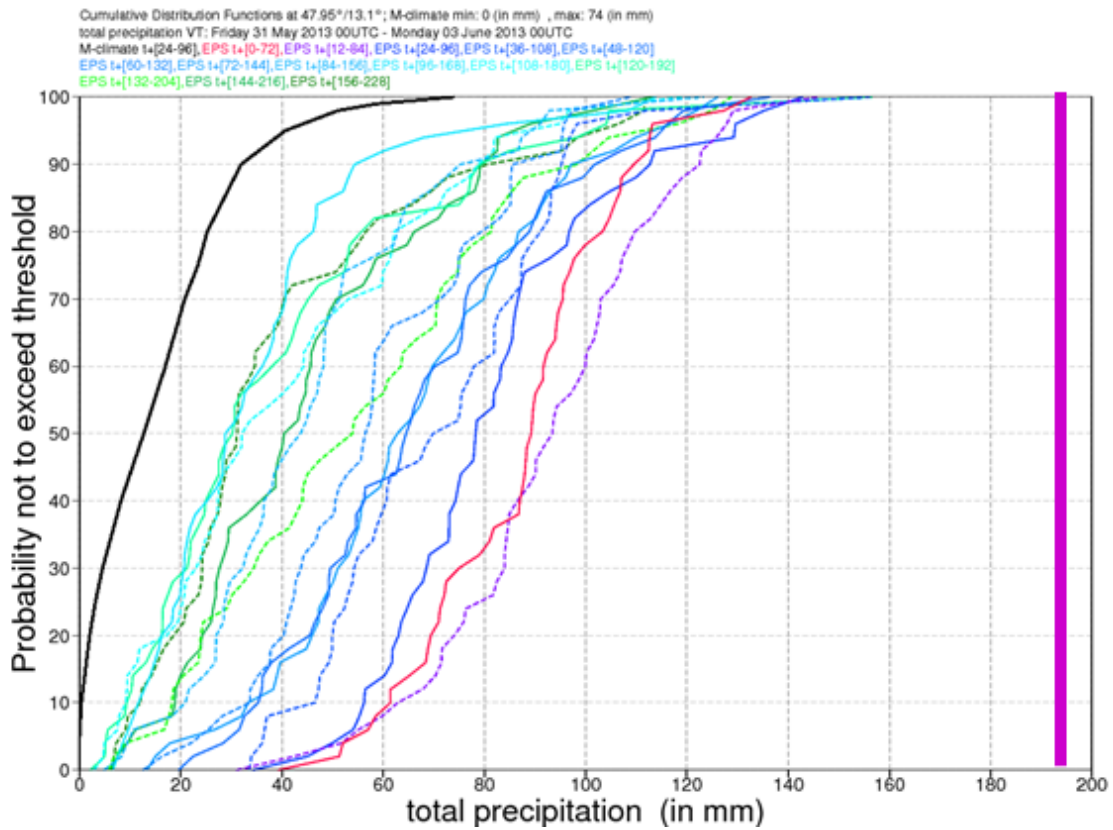


Figure 9. CDFs of total precipitation for Mattsee, Austria. The thick vertical magenta line denotes the reported rainfall, the black line indicates the model climate, and the other coloured lines show ensemble forecasts all valid for the same period.

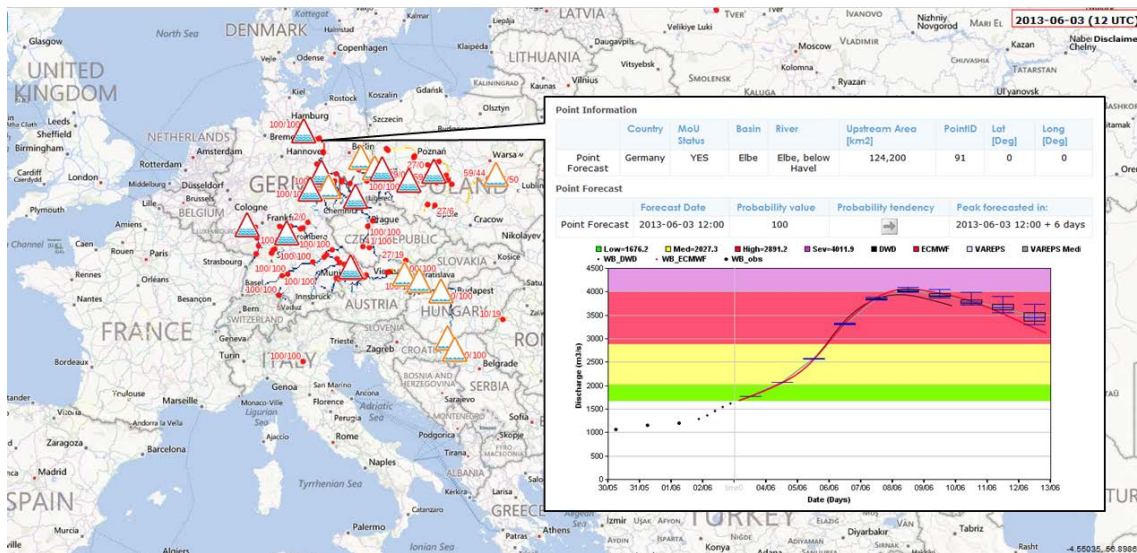


Figure 10. EFAS active alerts (red) and watches (orange) on 3 June 2013, and multi-model streamflow prediction for the Elbe River at Wittenberg, Germany.

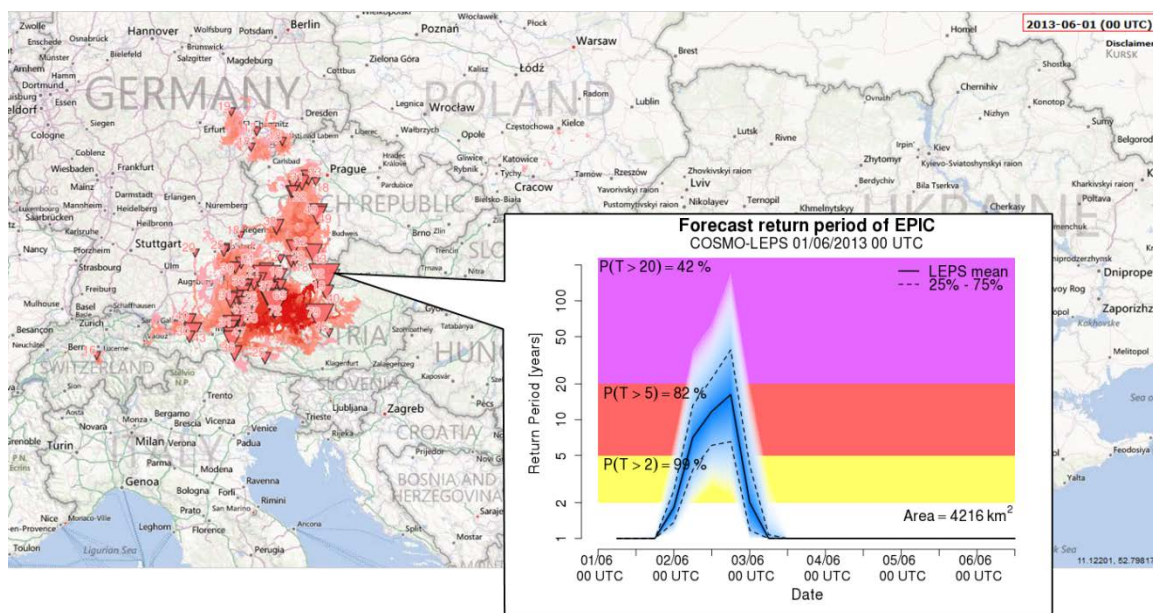


Figure 11. EFAS flash flood forecasts based on EPIC on 1 June 2013.

PBIAS [%] - 28/05/2013 to 20/06/2013 - LT = 7 days

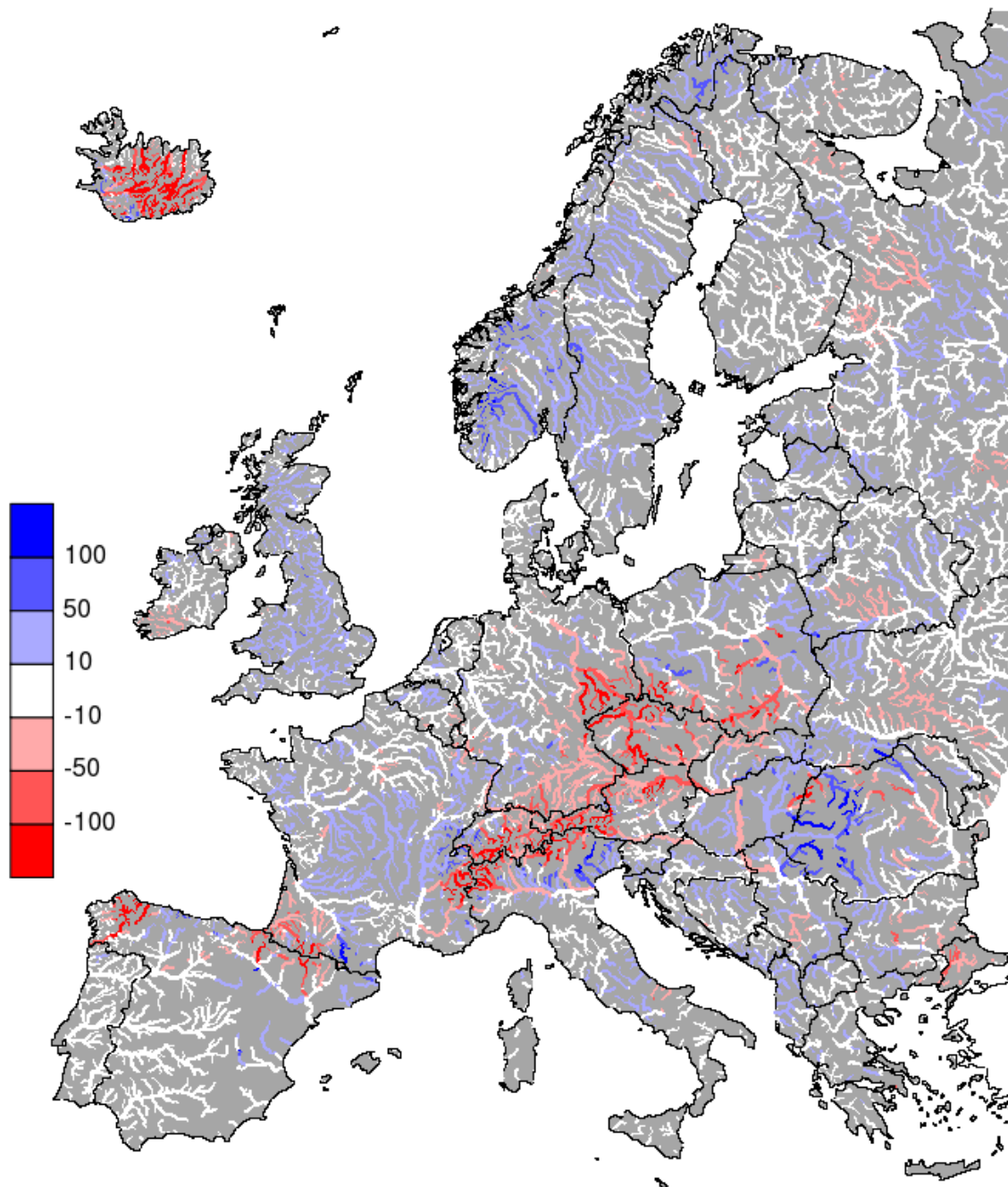


Figure 12. Percentage bias of streamflow for a lead time of 7 days calculated over the period 28 May-20 June 2013. The length of the period was chosen to capture both the rising and falling limb of the hydrograph associated with the event.

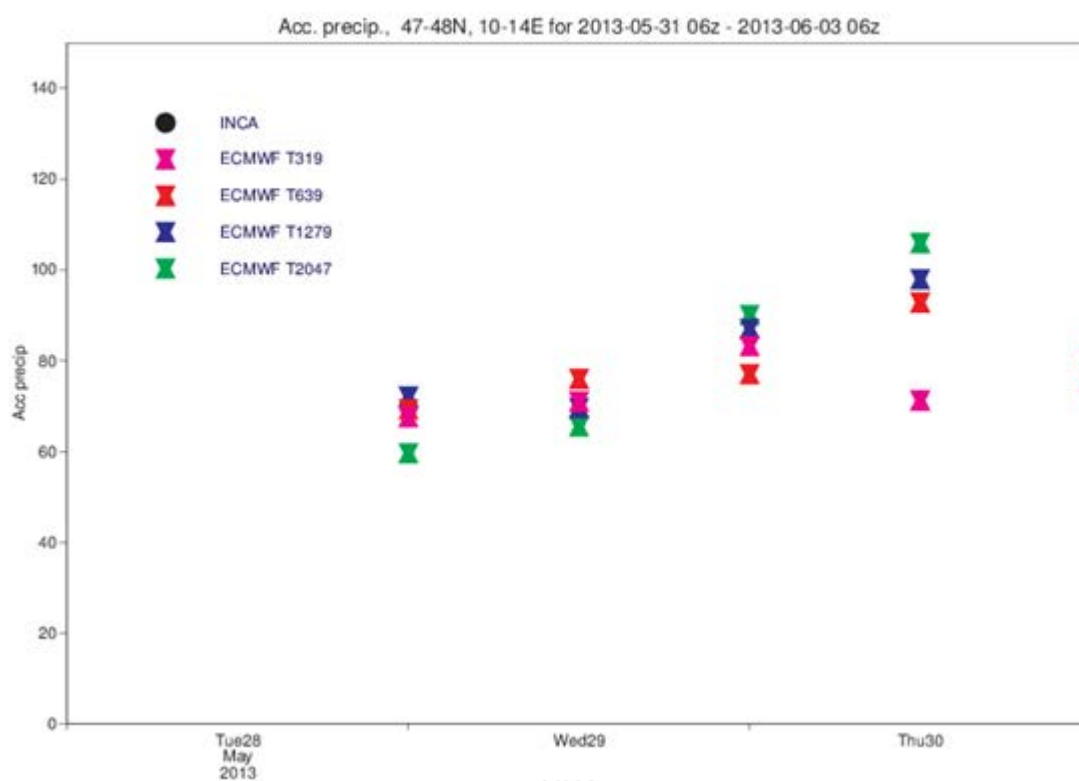


Figure 13. Accumulated precipitation in the 72-h period 31 May 2013 06 UTC – 3 June 2013 06 UTC averaged over the northern slopes area (47-48N, 10-14W, see Figure 3) from model runs at different resolution (represented by different colours), initialized at different times as indicated on the x-axis.

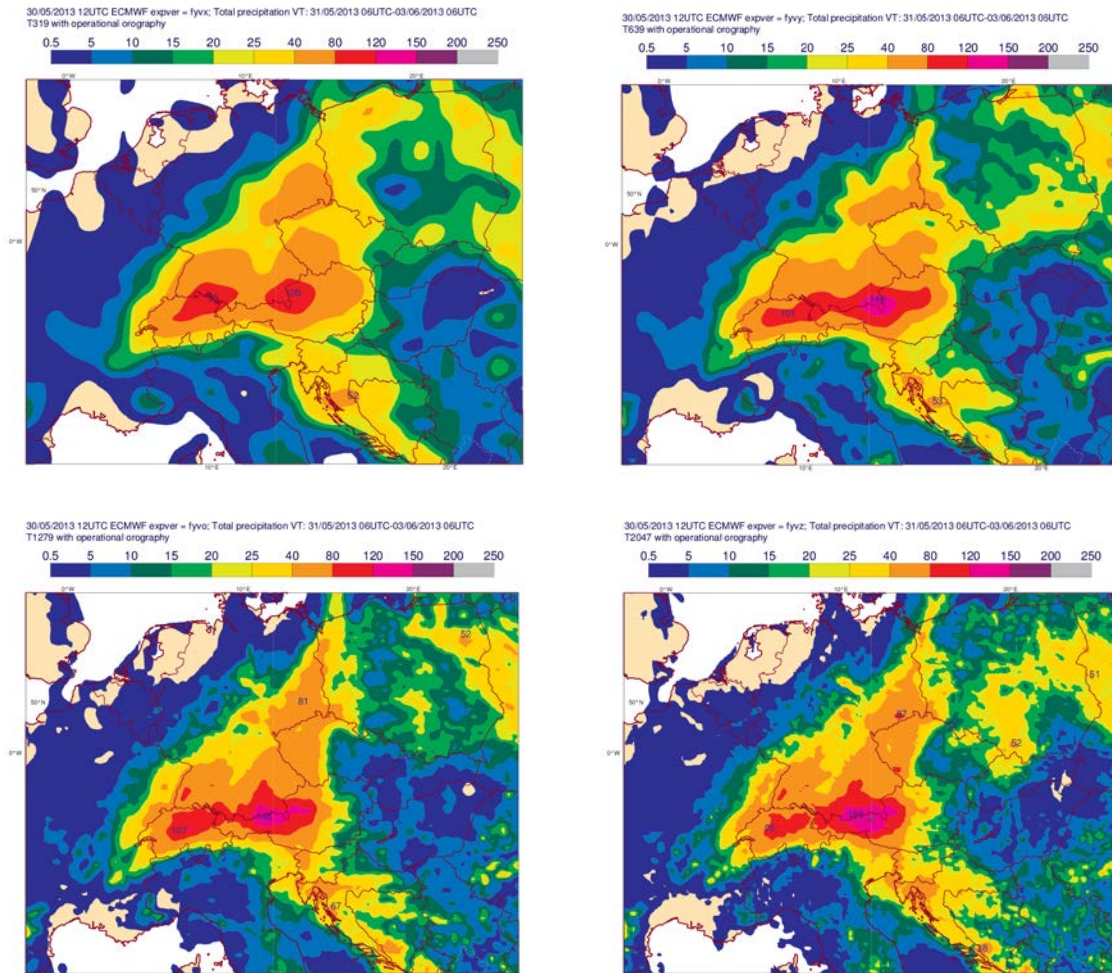


Figure 14. Precipitation amounts in the 72-h period 20130531 06 UTC – 20130603 06 UTC obtained from model runs at resolutions of 64 km, 32 km, 16 km, and 10 km, initialized at 20130530 12 UTC.

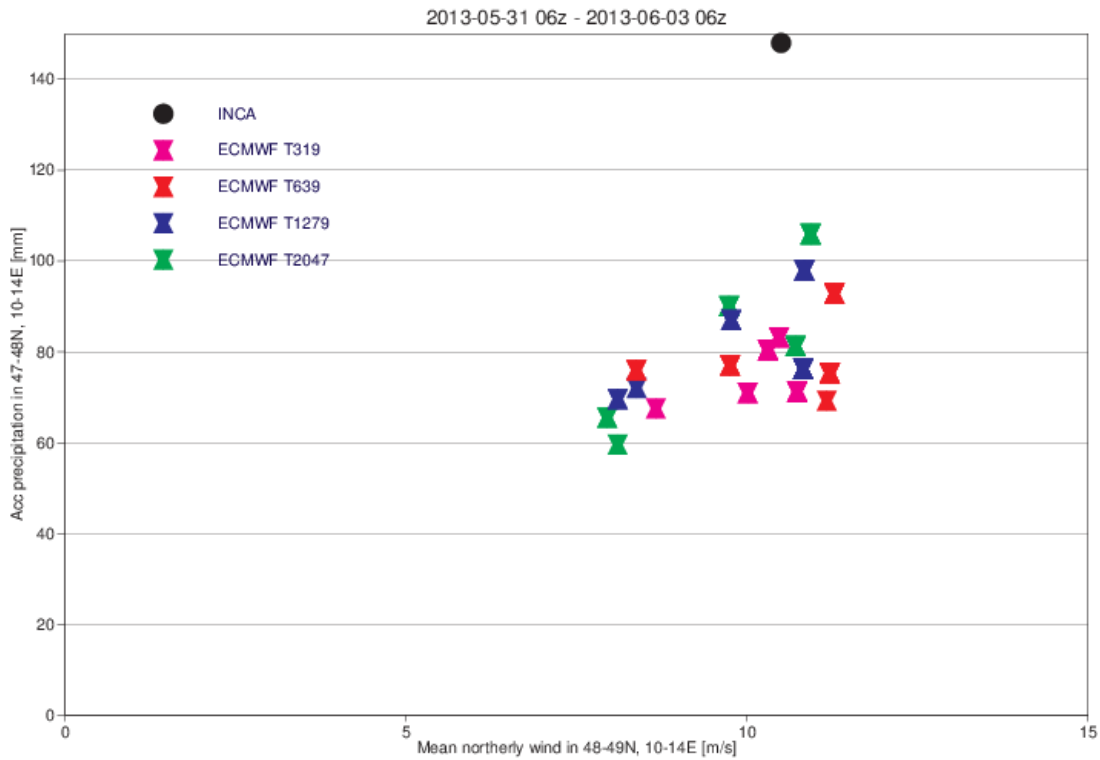


Figure 15. Relationship between forecast areal precipitation amounts averaged over 47N-48N, 10W-14W and the meridional wind component at 700 hPa, averaged over 48N-49N, 10W-14W (just to the north of the precipitation box) for the 72-h period 31 May 06 UTC to 3 June 06 UTC. Each cross represents one forecast, the black dot indicates the INCA analysis for precipitation and the ECMWF operational analysis (T1279) for wind speed.

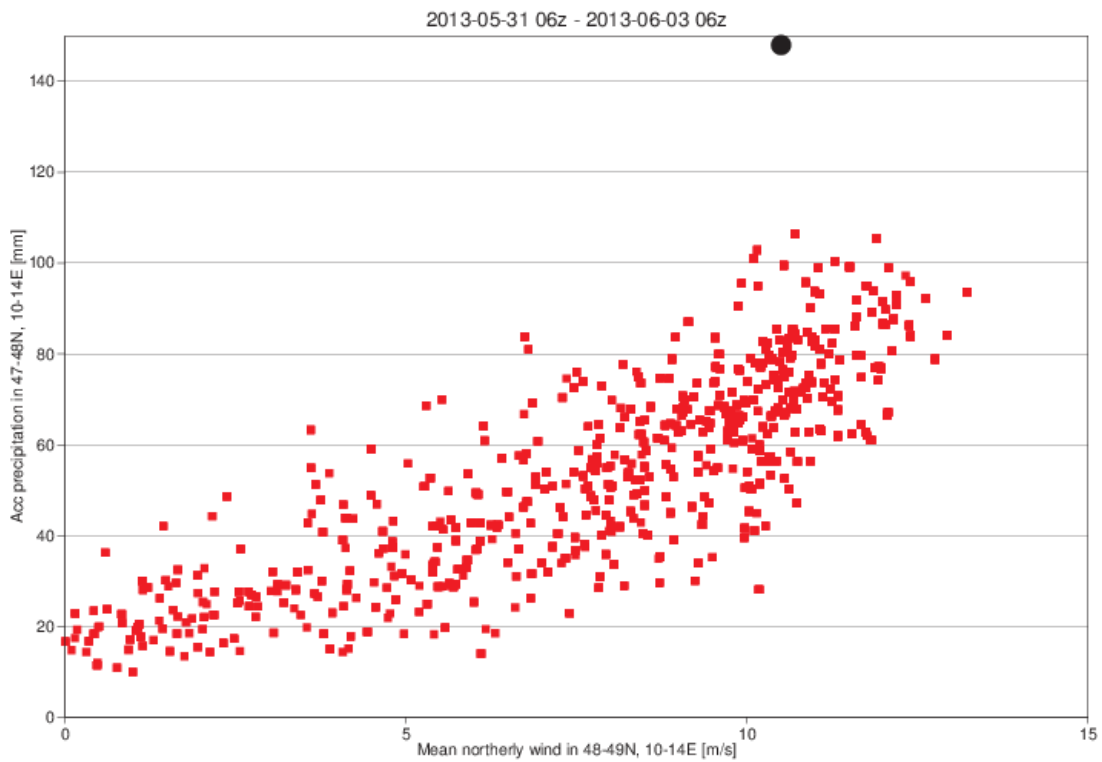


Figure 16. Same as Figure 15 but for each ensemble member from all forecasts initialized between 26 June and 31 June.

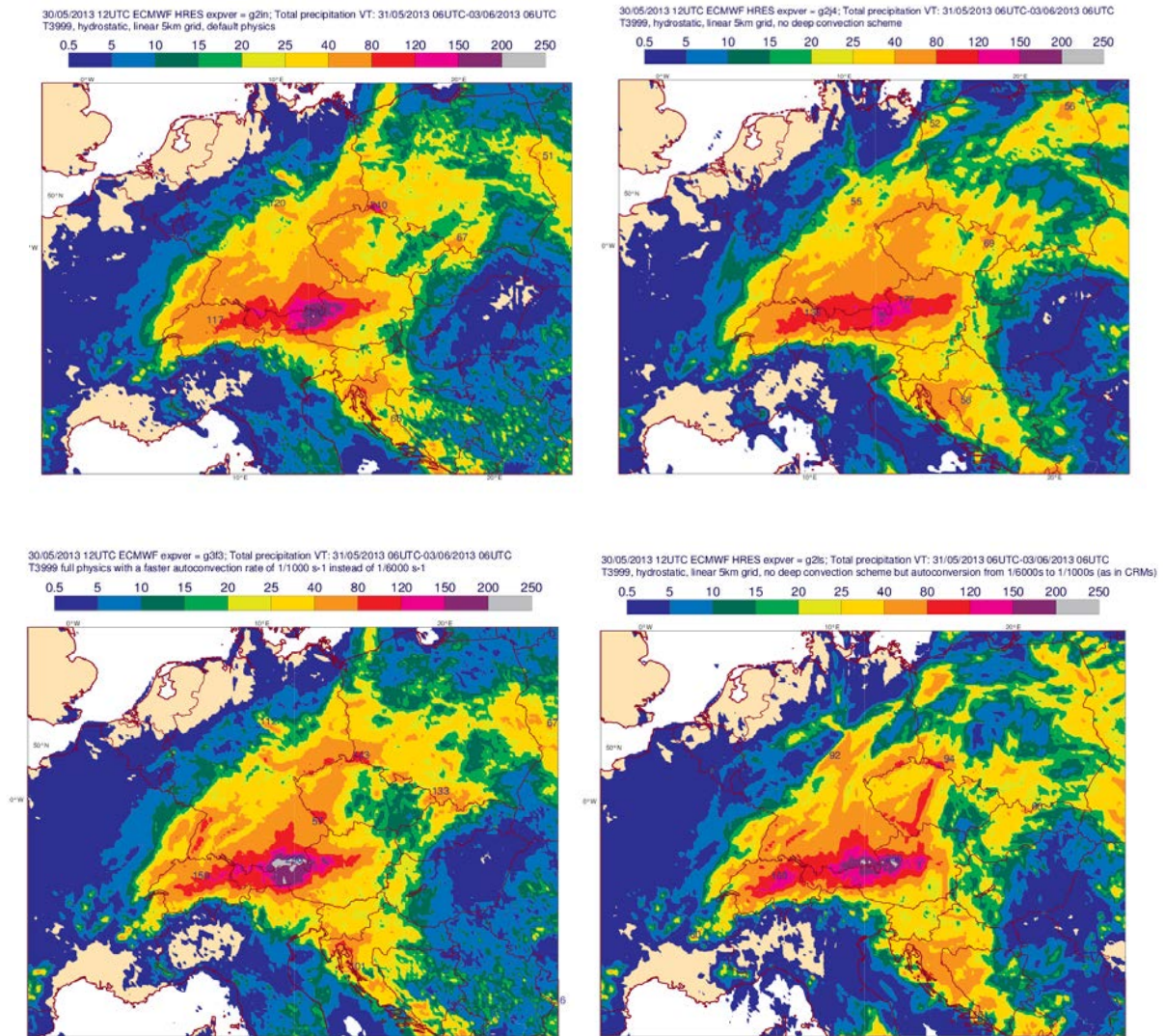


Figure 17. Precipitation amounts in the 72-h period 31 May 2013 06 UTC – 3 June 2013 06 UTC obtained from model runs at T3999 horizontal resolution with the deep convection scheme switched on (left), and switched off (right), with an autoconversion time-scale of 6000 s (top panels) and 1000 s (bottom panels). All forecasts were initialized at 30 May 2013 12 UTC.

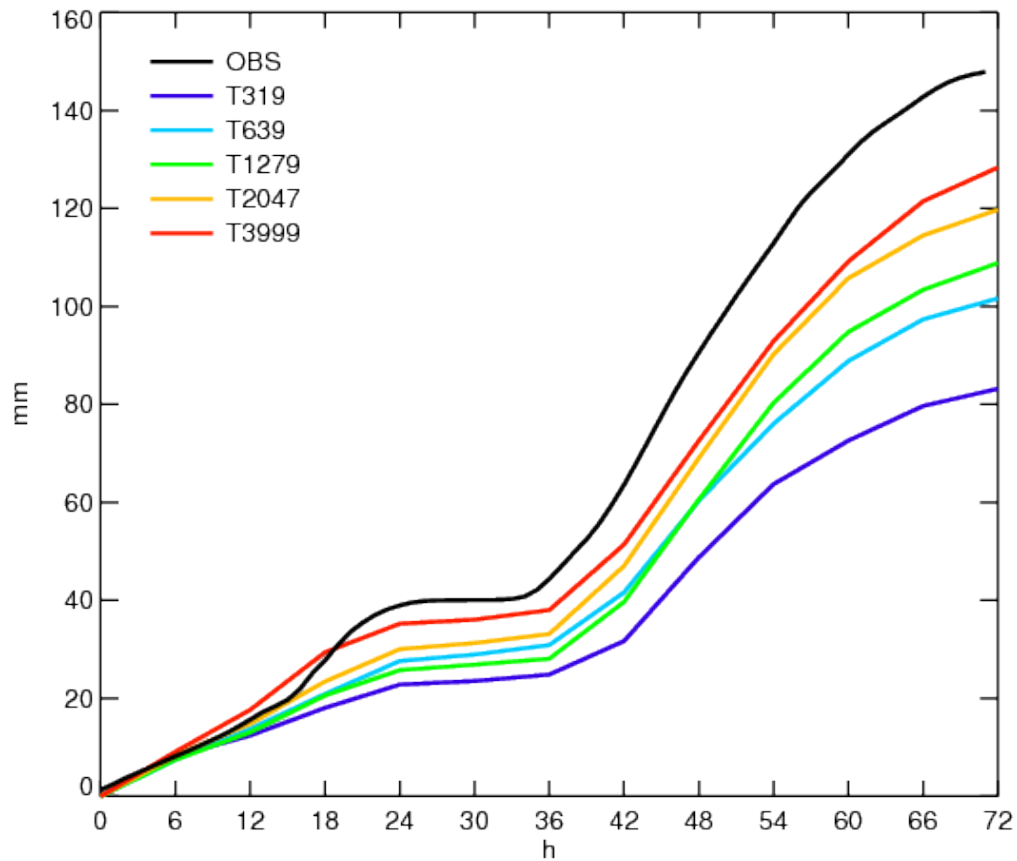


Figure 18. Cumulative precipitation in the alpine box 47N-48N, 10W-14W (Figure 3) for different ECMWF model resolutions. Observations show values from the INCA precipitation analysis. Time is given relative to 31 May 2013 00 UTC.

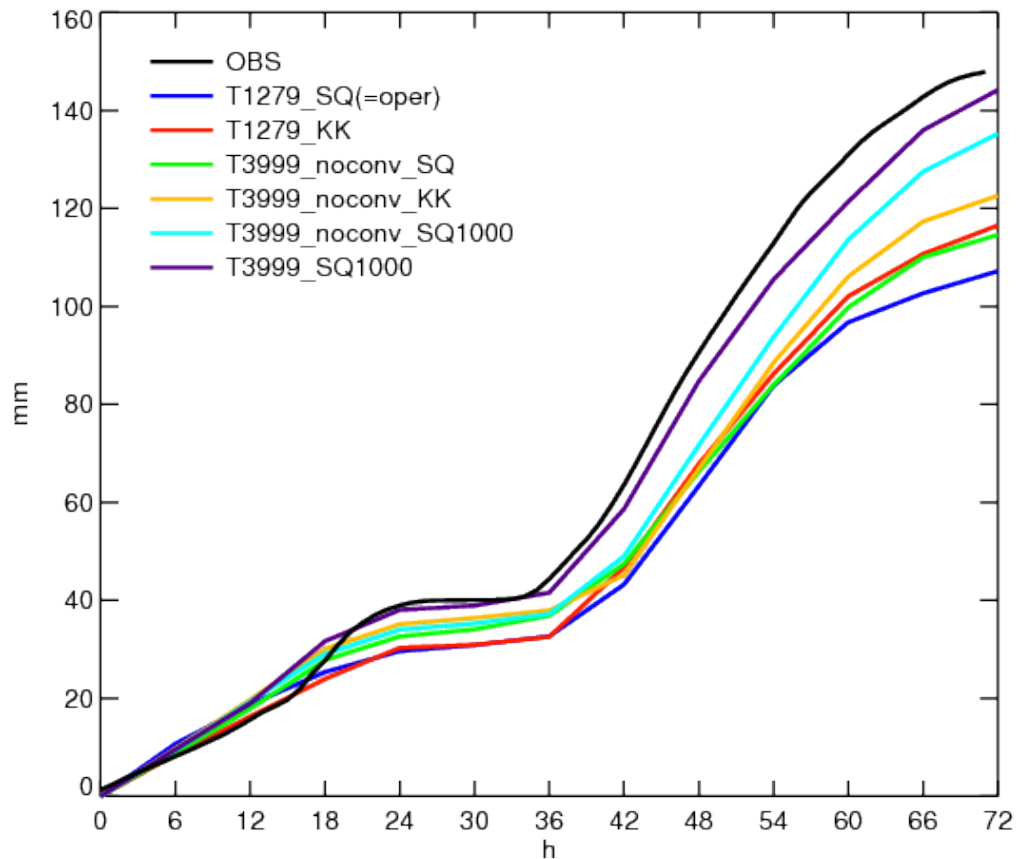
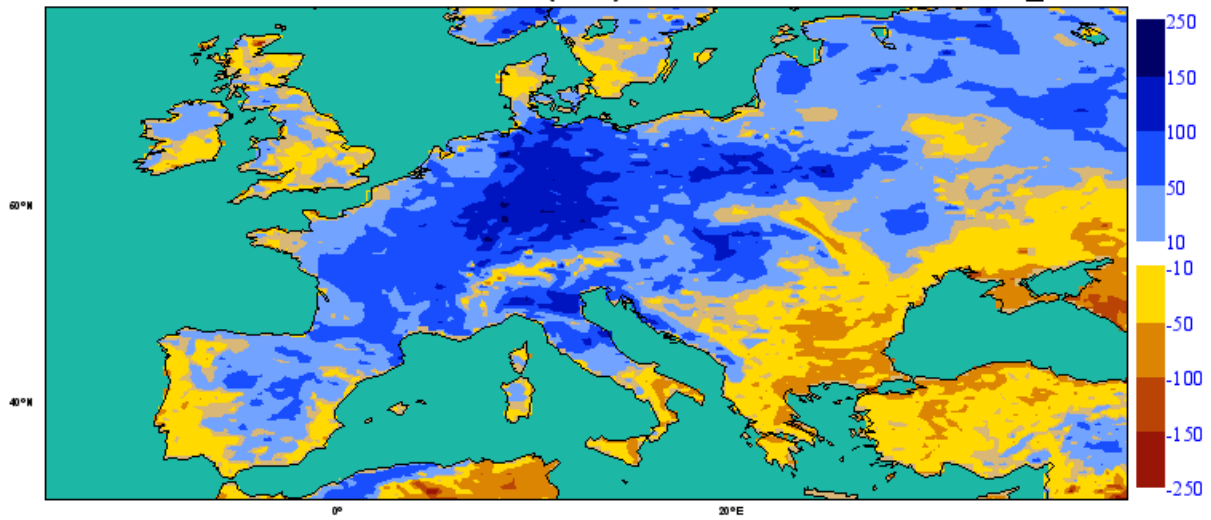


Figure 19. Cumulative precipitation in the alpine box (shown in Figure 3) for different formulations of the autoconversion+accretion process (SQ = Sundqvist scheme, KK = Khairoutdinov and Kogan scheme) at model resolutions T1279 and T3999. SQ1000 denotes the experiment where the autoconversion time-scale was reduced from 6000 to 1000 s; 'noconv' indicates that an experiment was run with the deep convection scheme turned off. Observations show values from the INCA precipitation analysis. Time is given relative to 31 May 2013 00 UTC.

**ECMWF root zone soil moisture (mm) 0529 to 0603: 2013 - 2008\_2012**



*Figure 20. ECMWF root zone (first metre of soil) soil moisture anomaly in mm, from 29 May to 03 June 2013 compared to the same 6-day period averaged over years 2008 to 2012.*

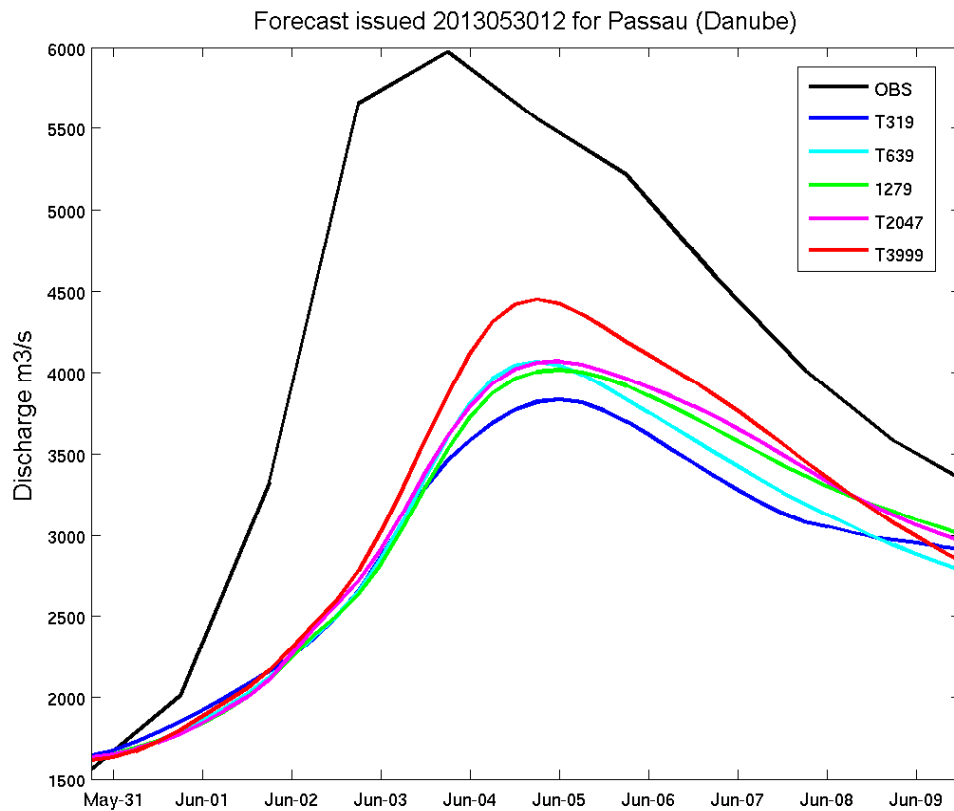


Figure 21. Forecasted discharge levels with different ECMWF resolutions for the station Passau at the river Danube. The black line denotes the simulated discharge using observed precipitation.

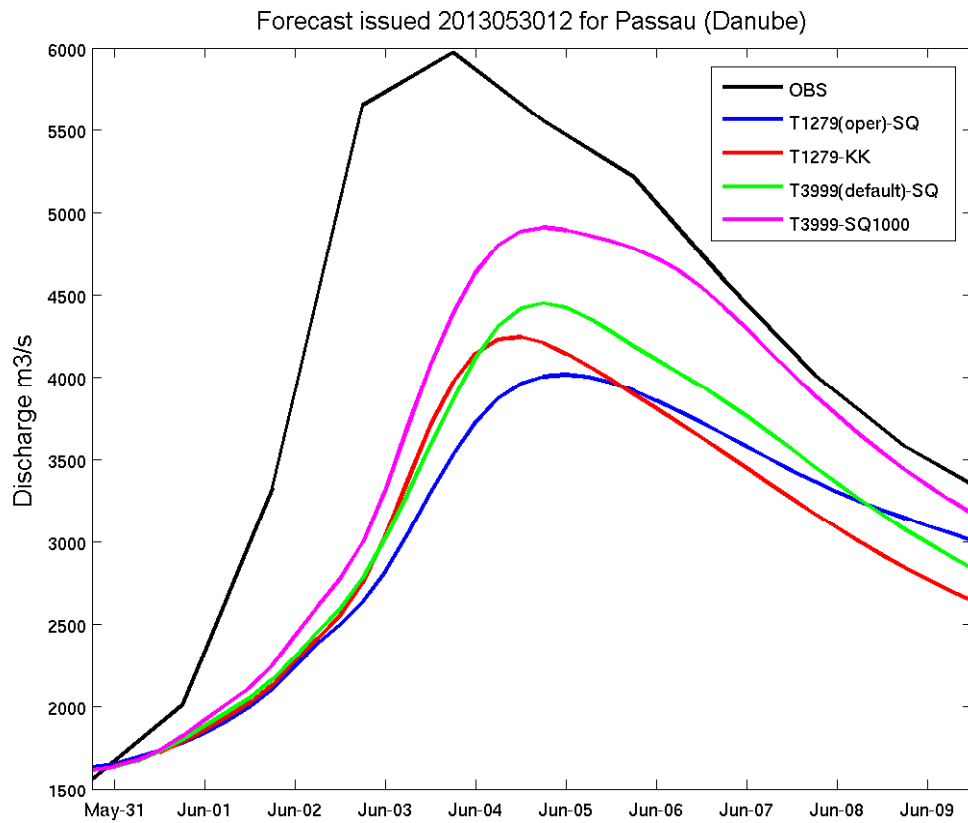


Figure 22. Forecasted discharge levels with two different model resolutions (T1279 and T3999) for the station Passau at the river Danube. The black line denotes the simulated discharge using observed precipitation, which can also be interpreted as the forecast potential.